Combination of two methodologies, artificial neural network and linear interpolation, to gap-fill daily nitrous oxide flux measurements

Laurent Bigaignon, Rémy Fieuzal, Claire Delon, Tiphaine Tallec

Combination of two methodologies, artificial neural network and linear interpolation, to gap-fill daily nitrous oxide flux measurements

Laurent Bigaignon[a,b], Rémy Fieuzal[a], Claire Delon[b], Tiphaine Tallec[a]

[a] *Centre d'Études Spatiales de la BIOsphère (CESBIO), Université de Toulouse, CNES/CNRS/INRA/IRD/UPS, 18 avenue Edouard Belin, 31401, Toulouse, France*
[b] *Laboratoire d'Aérologie (LA), Université de Toulouse, CNRS/UPS, 14 avenue Edouard Belin, 31401, Toulouse, France*

Keywords.

Greenhouse Gases, Soil, Chambers, Crops, Agriculture

Abstract.

Continuous N_2O flux acquisition is crucial to enrich our knowledge of the complex mechanisms underlying the annual greenhouse gas budget and to refine their estimation. N_2O flux measurement methodologies at high temporal resolution, i.e. micro-meteorology methodologies, are still scarce and may exacerbate the lack of important data, especially during the night if the required turbulent conditions are not met. The static and automated chamber methodologies also lead to numerous gaps in a time series due to low sampling frequency, hardware malfunctions, chambers removal during field operations or filtering of low-quality measurements. There is a strong need to define a generic and realistic N_2O flux gap-filling methodology, especially since there is no consensus on the methodology to be used.

In this study, we investigated the effect of using either the traditional linear interpolation methodology alone, either an Artificial Neural Networks (ANN) methodology alone or the combination of both on gap-filled daily N_2O flux dynamics and annual budget. All three methodologies were tested on daily N_2O flux time series measured with automated chambers

over 5 years from 2012 to 2016 on a southwestern France crop site following a wheat – maize rotation.

On average over the studied period, the results showed better statistical scores using the ANN methodology alone than using the linear interpolation methodology alone, with R^2 and RMSE of 0.84 and 12.4 gN ha^{-1} d^{-1} and of 0.68 and 17.4 gN ha^{-1} d^{-1}, respectively. However, whereas the use of ANN methodology reproduced well high measured N_2O fluxes, it induced overestimation on low measured N_2O fluxes where the use of the linear interpolation methodology was relevant. To overcome that issue and to take advantages of both methodologies we propose a new one which mixes both. On average, using the mixed methodology did not increase statistical scores compared to the ANN one, with a R^2 and a RMSE of 0.84 and 12.4 gN ha^{-1} d^{-1} respectively for both, but for periods with low measured N_2O fluxes using the mixed methodology improved the statistical scores and the observed daily flux dynamic.

1. Introduction

Nitrous oxide (N_2O) is an important greenhouse gas as it presents a high global warming potential, around 300-fold higher than carbon dioxide (CO_2), for an approximate residence time of 120 years in the atmosphere (Intergovernmental Panel on Climate Change (IPCC), 2013). Moreover, N_2O participates in stratospheric ozone depletion (Ravishankara et al., 2009). At the global scale, N_2O is responsible for 6% of the current global warming, its atmospheric concentration has increased at a rate of 0.93 ppb per year from 2007 to 2017 (WMO Greenhouse gas bulletin, 2018) and represents 46% of the total greenhouse gas (GHG) emissions from agriculture (United Nations Environment Program (UNEP), 2012). Agricultural soils constitute the main anthropogenic source of N_2O, mostly because of an increase in land conversion for agriculture and the intensified use of nitrogen fertilizers (Ussiri and Lal, 2013; Lognoul et al., 2017; Davidson, 2009; Snyder et al., 2009). The formation of N_2O in agricultural soils is mainly due to two microbial processes: nitrification and denitrification. Ammonium (NH_4^+) and nitrate (NO_3^-) concentrations together with soil water content, temperature, organic matter and pH, are the principal physical-chemical factors modulating the production of N_2O from agricultural soils (Hénault et al., 2005; Li et al, 2000; Parsons et al, 1993; Wiljer et Delwiche, 1954). N_2O emissions are thus determined by a combination of factors. The magnitude of each of these direct controls is subject to its own set of biological and abiotic controls (agricultural practices), showing the non-linearity of N_2O emissions.

In the aim of mitigating climate change by reducing N_2O emissions from soils, it is important to determine and understand N_2O flux dynamics in response to variability in the climate and agricultural practices. To this end, different technologies have been developed and it is common

to find studies with low sampling frequency for measuring N_2O fluxes. The static chamber method has been widely used (Reeves and Wang, 2015) as it presents the advantages of: (1) having low initial set-up costs, (2) being easily deployable from site to site and (3) being usable in small experimental plots, but it is also very demanding in manpower and offers a lower, more discontinuous sampling frequency than automated chambers (Zhang et al., 2014; Tellez-Rio et al., 2015; Reeves et al., 2016; Delon et al., 2017; Vinzent et al., 2017; Tallec et al., 2019). The use of a static chamber requires the operator to be well synchronized with N_2O flux events, which are not known a priori. Automated chambers have been developed to increase sampling frequency (e.g. four times a day) and to reduce the uncertainty related to temporal N_2O flux variability (Peyrard et al., 2016; Tallec et al., 2019). Nevertheless, due to field operations, instrument failure and/or quality control filtering, long periods of data loss may occur as for the static chamber method. Although the recent development of eddy-covariance methodology to measure N_2O fluxes (Nemitz et al., 2018) presents the advantage of sampling at very high frequency (with a half-hourly time step) and at larger scale (from several m^2 to several hectares) than with chambers, it also presents the disadvantage of losing a lot of data because of low turbulence, especially during the night (Tallec et al., 2019). So, whatever the methodology used, data loss is inevitable, which could be critical for studies of how the ecosystems function and for the calculation of annual N_2O budget. While standardized methodologies for CO_2 flux gap-filling (mean diurnal variation, look up table, regression application) are well recognized and validated thanks to clear, robust relationships between the fluxes and drivers, those for N_2O flux remain challenging and non-consensual (Nemitz et al., 2018). The methodologies applied are often site-specific and depend on the availability of ancillary data. A widely used gap-filling method in N_2O emission studies is the linear interpolation technique (Tellez-Rio et al., 2015; Vinzent et al., 2017). However, N_2O fluxes have high temporal variability (Tallec et al., 2019) and sporadic

events can lead to dynamics totally different from the smoother diurnal variation observed for CO_2. N_2O flux dynamics are too complex to use the same gap-filling methodology as that applied for CO_2 fluxes. Low sampling frequency of N_2O fluxes combined with a linear interpolation gap-filling method may thus result in the real N_2O flux dynamics being missed, under- or overestimation of the annual N_2O budget and misinterpretation of the effects of climate and management.

To overcome this issue, and in the context of the ICOS (Integrated Carbon Observation System; Franz et al., 2018) network, Nemitz et al. (2018) suggested using and testing the Artificial Neural Networks (ANN) methodology that had proved to perform well for CH_4 and CO_2 flux gap-filling (Papale and Valentini, 2003; Melesse and Hanley, 2005; Moffat et al., 2007, Dengel et al., 2013). Moffat et al. (2007), who reviewed 15 different techniques tested on a dataset compiled from six different European forest sites to fill gaps in values of the half-hourly Net Ecosystem Exchange (NEE), showed that ANN had a consistently good gap-filling performance and low annual sum bias, with R^2 between 0.41 to 0.90, and recommended its use even in different ecosystems. Melesse and Hanley (2005) tested ANN to gap-fill hourly CO_2 fluxes from three different ecosystems (forest, wheat, grassland) in the United States. They found that this technique could successfully predict observed values with R^2 values between 0.75 to 0.94 and therefore considered it reliable, efficient and highly significant to estimate CO_2 fluxes. However, the very fleeting N_2O fluxes are more difficult to simulate and gap-fill as, unlike CO_2 fluxes, they do not present any diurnal dynamics (Tallec et al., 2019). ANN is a statistical method that provides a relatively easy way to approach non-linear functions. It has the advantage of being usable without any knowledge of the processes that have an impact on the targeted variable(s). Some knowledge on the key drivers for thematic applications, as for N_2O fluxes gap-filling, is still needed. Today, few studies have used and evaluated the performance of ANN methodology

111 with other methodologies simulating N_2O fluxes (Ryan et al., 2004; Villa-Vialaneix et al., 2012;
112 Taki et al., 2018). Ryan et al. (2004) undertook to simulate daily N_2O emissions from an intensive
113 grassland ecosystem in New Zealand using ANN methodology and obtained good statistical
114 results, with R^2 ranging from 0.67 to 0.85. Taki et al. (2018) compared the use of ANN and linear
115 interpolation methodologies to gap-fill a 6 years time series of N_2O flux measured on a Canadian
116 crop site following a corn/soybean/winter wheat rotation. On average, whatever the cropping
117 year, they found a lower R^2 with the use of ANN than Ryan et al. (2004). Depending on the
118 cropping year and the crop species, R^2 ranged from 0.19 (for a soybean crop) to 0.65 (for a maize
119 crop). This strong variation in the ANN performance may question the relevance of using that
120 methodology and underlines the need to more investigate it in different context and
121 configuration. However, Taki et al. (2018) recommended the use of ANN instead of the classical
122 interpolation method, as on average the former scored a higher R^2 (0.41) than the latter (0.34)
123 when considering the entire studied period.
124 The study proposed here is part of this dynamics, as comparisons between gap-filling
125 procedures on N_2O fluxes are still lacking. Its objectives are twofold: (1) to evaluate and compare
126 linear interpolation and ANN as gap-filling methodologies to reproduce daily low and high N_2O
127 fluxes and (2) to propose a third gap-filling approach combining both methodologies using a
128 criterion on the method's choice, either linear interpolation or ANN, based on the duration of the
129 missing data period and the N_2O flux magnitude. All three methodologies were tested on a long
130 time series of measurements taken on an agricultural plot (maize/wheat rotation) in the south-
131 west of France from 2012 to 2016 and compared together according to each crop plot functioning
132 period (bare soil, growing season, low or high N_2O fluxes intensity, etc.). The effect of the
133 methodology's choice on the estimated annual N_2O budget is discussed.
134

2. Materials

2.1 Experimental site

The study is based on a dataset collected at the Lamasquère site (FR-Lam) in the South West of France (43°29’47’’N, 1°14’16’’E, 180 m elevation). This crop site is part of an experimental dairy farm (Domaine de Lamothe, Instituts Nationaux Polytechniques). The site is located in a plain having an oceanic climate with Mediterranean and continental influences, a mean annual rainfall of 680 mm and a mean annual temperature of 12.6 °C. The soil is mainly clayey (50.3% clay, 35.8% silt, 11.2% sand, 2.8% organic matter). The plot is located near the river Touch, a tributary of the river Garonne, in the Adour-Garonne water catchment area.

This experimental plot is part of the Regional Spatial Observatory, the regional ZA PYGAR (Zone Atelier Pyrénées-Garonne), the national research infrastructure OZCAR (Critical Zone Observatories: Research and Applications; Gaillardet et al., 2018) and the European network ICOS (Integrated Carbon Observation System). The site is therefore fully equipped with instruments to monitor greenhouse gas fluxes, meteorological, radiation and soil variables (Béziat et al, 2009; Tallec et al, 2013). Vegetation dynamics are also monitored in detail with green area, biomass and height measurements.

Management of the crop plot is intensive, with exportation of all aboveground biomass for mulching the cowsheds and/or feeding the herd. An annual irrigation of approximately 150 mm is applied when maize is cultivated. The total amount of nitrogen (N) applied varies from 100 to 200 kgN ha^{-1} and 110 to 145 kgN ha^{-1} for mineral and organic fertilization respectively. Input modalities vary according to the crop species. Mineral fertilization is split into 3 applications for wheat and applied once for maize. The FR-Lam site occupation followed the rotation maize (2012), wheat (2013), cover crop (CC) (2013), maize (2014), maize (2015), wheat (2016), CC (2016).

159

160 *2.2 N_2O flux measurement*

161 To measure N_2O emissions, 6 stainless steel automated chambers (covering an area of 0.161
162 m^2) were installed on the plot according to a closed dynamic set-up. The chambers were
163 elongated (70cm×23cm×10cm) so as to be easily inserted in the crop inter-rows, where they were
164 placed at a 10 cm soil depth. A previous comparison study between automated chambers and
165 eddy-covariance methodologies (Tallec et al. 2019) on the same site showed that a set of 6
166 automated chambers was sufficient to integrate spatial heterogeneity of the site and to well
167 capture the mean daily N_2O flux dynamics. The set-up measured N_2O accumulation in each
168 chamber alternately during 17.5 minutes every 6 hours, i.e. four cycles a day (00:00, 06:00,
169 12:00, 18:00). A pump maintained continuous air circulation in and out of the chamber at a
170 constant flow rate (1 $L.min^{-1}$). Sampled air was supplied from the chamber to a gas analyser that
171 measure N_2O molar fraction every 10 seconds (Thermofisher 46i, Megatec, France). The
172 calculated N_2O fluxes (exponential fitting) were filtered by means of a mixture of goodness-of-fit
173 statistics and visual inspection (Tallec et al., 2019). A fan also enabled air homogeneity in the
174 chamber.

175 Daily N_2O fluxes were calculated as the mean value of all available fluxes during the day.
176 The choice to work at a daily timescale was made as no significant diurnal N_2O flux intensity
177 variation was found on FR-Lam site in a previous study (Tallec et al., 2019). Because of
178 hardware dysfunction and/or technical operations, such as tillage and harvest, chambers were
179 removed many times, leading to missing data which means that the number of available N_2O flux
180 measurement per day to calculate a daily N_2O flux varied from 0 to 24. In this study, in order to
181 maximize the size of the dataset for the need of that study we kept all available daily fluxes, even
182 if calculated with only one measurement a day. Finally, from 2012 to 2016, out of 1827 daily

183 N_2O flux values, 1442 were acquired. The whole dataset included 63% of "highly" representative
184 daily values (calculated with 12 to 24 measurements a day), 22% of "moderately" representative
185 daily values (calculated with 6 to 12 measurements a day) and 13% of potentially "poorly"
186 representative daily values (calculated with 1 to 6 measurements a day).
187
188 *2.3 Meteorology, soil variables and ancillary data measurements*
189 The rich dataset acquired on FR-Lam offers the possibility to test different combinations of
190 possible explanatory variables for the input layer in the ANN and to choose the most explanatory
191 (see section 3.1.2.3). Matter and energy fluxes, meteorological data, radiation and soil variables
192 were available at a half-hourly time step and are described in Table 1. The measurement
193 methodology for each variable is described in Beziat et al. (2009) and Tallec et al. (2013). Each
194 variable was aggregated at a daily time scale. Vegetation data were collected from 5 to 6 times a
195 year during the growing season and a simple linear interpolation was applied to obtain the daily
196 dynamics.
197

198

Variable names	Variable description (unit)
ABG	Above Ground Biomass (kg m^{-2})
E	Measured Evapotranspiration (kg m^{-2} d^{-1})
ETP	Potential Evapotranspiration (mm)
GPP	Green Primary Production (gC m^{-2} d^{-1})
H	Sensible heat flux (watt m^{-2} d^{-1})
h_veg	Vegetation height (m)
LAI	Leaf Area Index (m^2 m^{-2})
LE	Latent heat flux (W m^{-2} d^{-1})
LW	Incoming long wave (W m^{-2} d^{-1})
NEE	Net Ecosystem Exchange (gC m^{-2} d^{-1})
P	Rain (mm)
Pa	Pressure (kPa)
PPFD	Photosynthetic Photon Flux Density (µmol m^{-2} d^{-1})
PWC	Plant Water Content (%)
Reco	Ecosystem respiration from soil (gC m^{-2} d^{-1})
RH	Relative humidity (%)
Rg	Global radiation (MJ m^{-2} d^{-1})
Rn	Net radiation (W m^{-2} d^{-1})
SWC	Soil Water Content at 0, 5, 10, 30, 50 and 100 cm (%)
Ta_max	Maximum air temperature of the day (°C)
Ta_mean	Mean air temperature of the day (°C)
Ta_min	Minimum air temperature of the day (°C)
Ts	Soil temperature at 0, 5, 10, 30, 50 and 100 cm (°C)
Waterfall	Daily rain and irrigation event (mm)
WS	Wind speed (m s^{-1})

199 **Table 1**. Description of variables potentially available for gap-filling

200
201

Unfortunately, soil mineral nitrogen content was not available for all years and with low temporal resolution. Thus, to include the fertilization effect on N_2O emissions in the ANN construction, a decreasing exponential function $\boldsymbol{N_t}$ (Eq. 1) was developed to account for the effect of fertilizer on N_2O fluxes. The choice of coefficient 0.10 was determined based on the visualisation of the function's temporal dynamic. The aim of this function is to memorize a fertilisation event over multiple days after a fertilisation as we noticed, based on observations, that N_2O fluxes appears several days after a fertilisation event if the environmental conditions are met. No optimisation process was undertaken to find the most accurate coefficient value.

$$N_t = N_0 \times e^{-0.10*t} \quad (1)$$

Here $\boldsymbol{t}$ represents the number of days after fertilization, $\boldsymbol{N_t}$ is the nitrogen function value at day $\boldsymbol{t}$ after fertilization (kgN ha^{-1}) and $\boldsymbol{N_0}$ is the quantity of nitrogen fertilizer applied by the farmer on day 0 (kgN ha^{-1}).

3. Methods

3.1 ANN gap-filling methodology

3.1.1 General principle

In this study, the ANNs created are based on the algorithm proposed by Bishop (1995) (i.e., multi-layer perceptrons implemented in the nnet R package) and are composed of three layers of neurons (input, hidden and output) connected by synapses (Fig. 1). The input layer represents the predictive variables selected by the user to explain the targeted variables of the output layer. The number of input parameters and hidden neurons is determinant in the creation of a neural network and to avoid over fitting. Not enough hidden neurons will make it difficult to reach an accurate

estimation of the targeted variable, while too many will lead to noisy estimates (Delon et al., 2007). The relationship between input and output variables is modelled by sigmoid functions connecting neurons, the weights of interactions being determined through an iterative procedure.

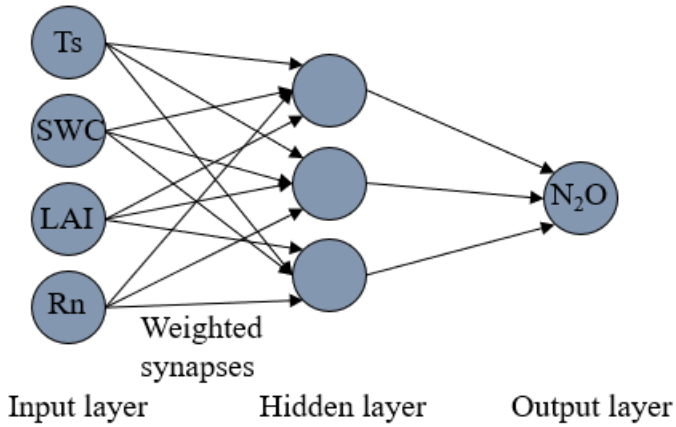

Fig. 1. Schematic MLP with 4 input variables, 3 hidden neurons and 1 output variable

During the model training, nnet uses supervised learning algorithms. The synapse weights are modified to fit the network in order to reduce an error function (i.e., Sum of Squared Errors (SSE)) corresponding to the difference between predicted and observed output (Guenther and Fritsch, 2010; Ryan et al, 2004) following the Broyden-Fletcher-Goldfarb-Shanno algorithm. The values of the weights are initialized with random values and progressively adjusted.

3.1.2 Creation of the neural network step by step

3.1.2.1 Neural Network performances

The data preparation procedure is established in accordance with the following studies Lek et al. 1966 and Olden et al. 2002, which recommend: (1) to standardize the measurement scales of the network inputs (by subtracting the mean value and dividing by the standard deviation) especially when the measurements are of different orders of magnitude, and (2) to convert the

range of the output variable to the interval [0-1] to conform to the interval of variation of the sigmoid transfer function (by subtracting the minimal value and dividing by the range of variation).

After normalization, the data set was randomly partitioned into two independent sets of equal data amount, 50% of the data to train and 50% of the data to test the created ANN, that enables to test the ANNs generalisation efficiency on an important amount of data. This 50/50 partitioning operation was repeated 40 times with the objective of obtaining 40 different random draws and selecting the draw with the highest performance.

The performance levels of the ANNs were evaluated using the determination coefficient (R^2, Eq. 2.), the Root Mean Squared Error (RMSE, Eq. 3.) and the Relative Root Mean Squared Error (RRMSE, Eq. 4.).

$$R^2 = \frac{(\sum_{i=1}^{n}(p_i - \bar{p}_i)(o_i - \bar{o}_i))^2}{\sum_{i=1}^{n}(p_i - \bar{p}_i)^2 \sum_{i=1}^{n}(o_i - \bar{o}_i)^2} \quad (2)$$

$$RMSE = \sqrt{\frac{\sum_{i=1}^{n}(o_i - p_i)^2}{n}} \quad (3)$$

$$RRMSE = \frac{RMSE}{\bar{y}} \times 100 \quad (4)$$

With n the number of observed values, o_i the observed value, p_i the predicted value and $\bar{o}$ and $\bar{p}$ the mean of observed and predicted data, respectively.

Different ANN configurations were tested. An overall neural network was implemented first on the whole dataset and then by discriminating each crop growing season and bare soil periods.

3.1.2.2. Early stopping procedure

In order to avoid over or under fitting during ANN training, an early stopping procedure was setup to determine the best number of iterations required to build the ANN model. For every 40

draws, ANNs were created and trained throughout 1 000 iterations and saved every 10 iterations (in total 4000 created ANNs for one functioning period). Then the 4000 trained ANNs were tested on the testing datasets. The R^2 and RMSE between observations and simulations on the training and testing dataset were also saved every 10 iterations for the 40 draws. The number of required iterations to build the best ANN model and select the best draw was determined in function of the minimum value of RMSE obtained on the testing datasets. Fig. 2 illustrates the case of draw number 5 for maize 2012 period.

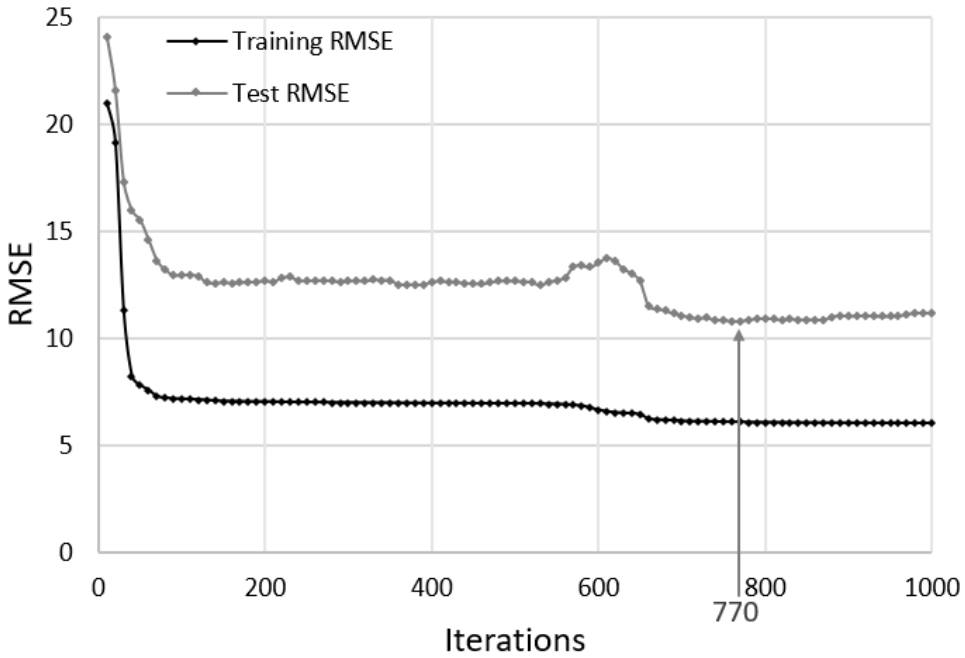

Fig. 2. RMSE (gN ha^{-1} d^{-1}) between ANN training (black) and testing (grey) datasets in function of iterations for draw number 5 during maize 2012 period. Here the minimum RMSE for the test simulation is reached after 770 iterations.

For that draw, the ANN created after 770 iterations was selected as it corresponds to the minimum RMSE of the testing dataset. Below or above that value the ANNs may be under or overfitted.

The best ANN determined from the iteration procedure was then kept and saved for every 40 draws of each functioning period. Then a classification of the 40 random draws was done in function of R^2 in order to select the draw showing the best R^2. A final test to select the best ANN for a functioning period was then made by comparing the ANN simulation on the test dataset with the corresponding observations dynamic. If this visual dynamic comparison was not satisfying, the second ANN and draw set with the best R^2 result was chosen, and so on.

3.1.2.3 Selection of input variables

The methodology used to select the most appropriate combination of variables for each period is presented in Fig. 3. Only input variables (Table 1) without any missing values were considered. A linear regression calculation between each variable and N_2O fluxes was then performed to select a combination of variables showing the highest correlation with N_2O fluxes (highest R^2 values). Afterwards, numerous ANNs were created by testing different combinations of the selected variables for each functioning period. The final input combination was selected based on the previously described process using the criterion R^2, RMSE and visual checking. Finally, a specific ANN was built for each functioning period using a combination of 4 or 5 input variables, and 3 hidden neurons to fit the output variable, i.e. the daily soil N_2O fluxes. Increasing the number of input parameters and/or hidden neurons did not improve the results significantly (data not shown).

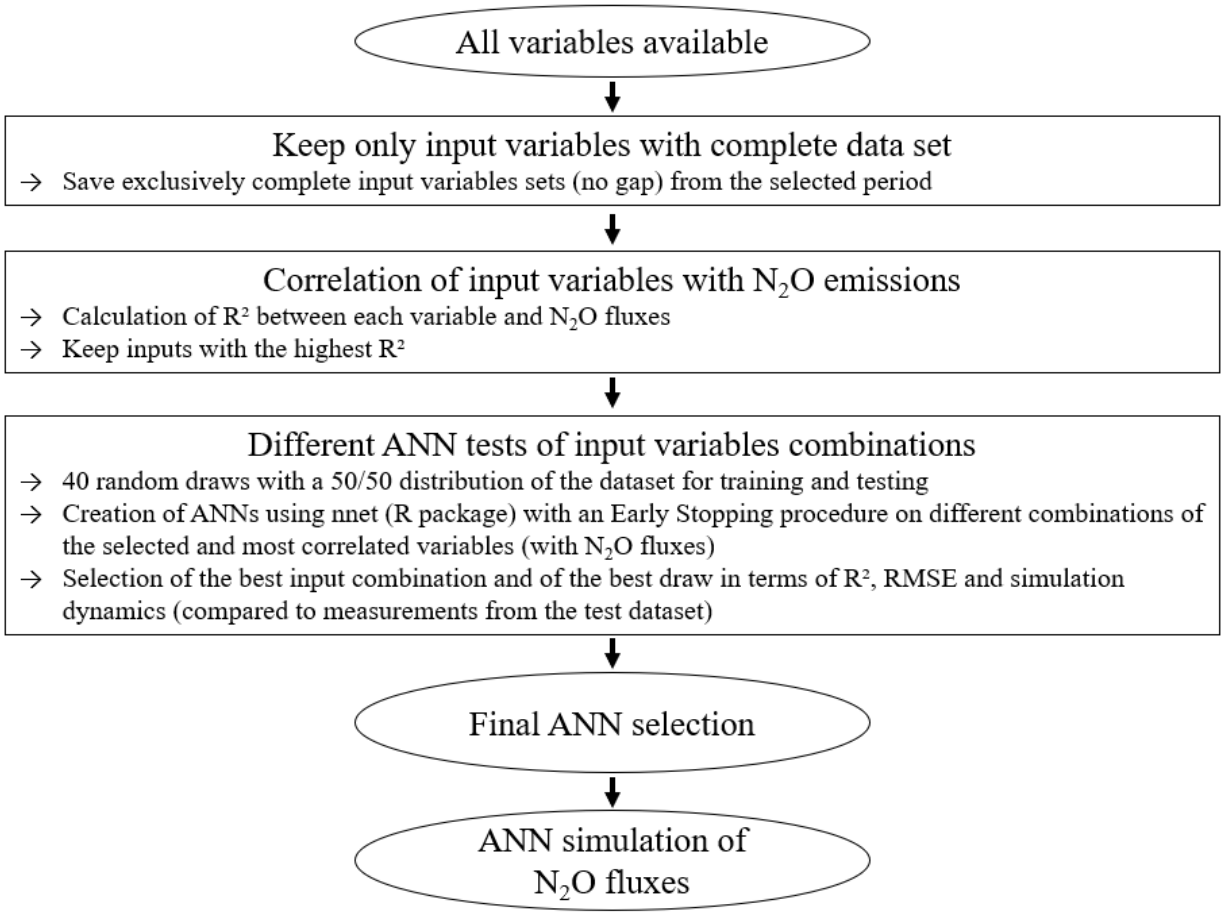

Fig. 3. Diagram outlining the successive steps to implement the ANN methodology.

3.2 Comparison between ANN and linear interpolation gap-filling methodologies

In order to evaluate the linear interpolation methodology and compare it with the ANN methodology on exactly the same days of observations, artificial gaps were created into the dataset used for the testing procedure (Fig. 4) for each functioning period. Each artificial gap was then filled using the linear interpolation method between the surrounding training values. The linear interpolation methodology was evaluated statistically using the same indices as described in section 3.1.2.1 (R^2, RMSE, RRMSE).

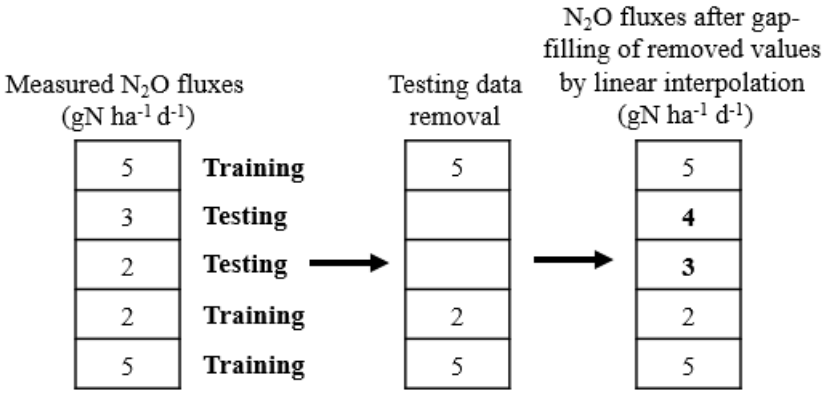

Fig. 4. Method used to create and linearly interpolate artificial gaps from the N_2O observations.

3.3 Determination of the GMD (Gap Magnitude and Duration) coefficient

The comparison between ANN and linear interpolation methodologies showed that each technique may have benefits and limitations depending on the gap condition (see section 4.5). Therefore, the best gap-filling approach would be to combine the two techniques with the help of a new criterion, the coefficient GMD (Eq. 5) which would allow the most suitable methodology to be chosen. The value of GMD depends on the length of the gap and on the difference between the N_2O fluxes intensity bracketing the gap. GMD thus allows the best gap-filling methodology to be chosen between linear interpolation and ANN.

$$GMD = D * abs(FN_2O_{before\ gap} - FN_2O_{after\ gap}) \quad (5)$$

Where D is the number of consecutive missing days in the gap and $FN_2O_{before\ gap}$ and $FN_2O_{after\ gap}$ are the N_2O flux values observed at the beginning and the end of the gap, respectively.

A decision tree to guide the choice to use either the linear interpolation or the ANN gap-filling methodology to fill a specific gap, depending on the GMD value, is developed in Fig. 5.

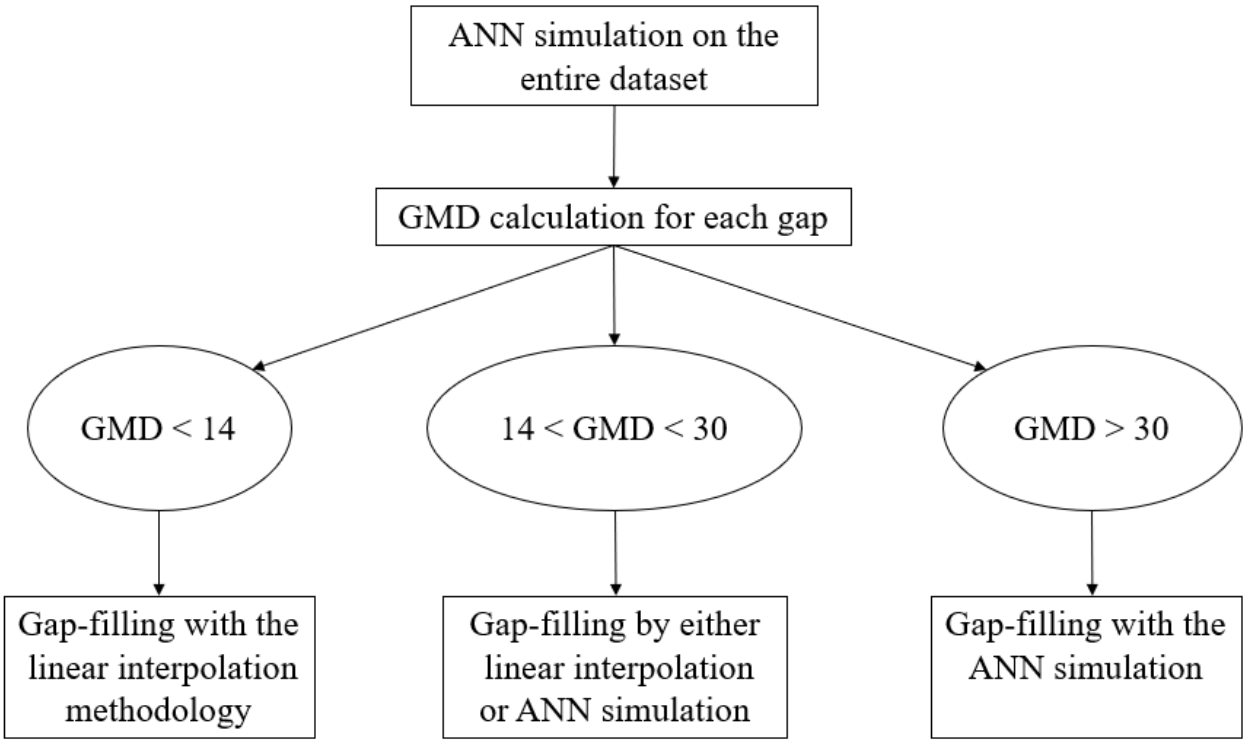

Fig. 5. Decision tree helping to select the more suitable gap-filling method according to GMD value.

3.4 Estimating annual N_2O budget uncertainty due to gap-filling

The uncertainty of the annual N_2O budget related to the gap-filling was investigated using a methodology adapted from Richardson and Hollinger (2007). This methodology is usually used to estimate annual NEE gap-filling uncertainty (Richardson and Hollinger, 2007; Schmidt et al., 2012). It is calculated by adding random gaps as actually observed in each real site–year of data gaps and then by adding small and long gaps (the maximum gap length is 8 days). However, in this methodology, the data set specificity is not taken into account, i.e. the number, length and locations of gaps are not respected. To include this information, a new methodology was

proposed as follows (Fig. 6): (1) the N_2O datasets were first gap-filled according to each functioning period by using the combined methodology exposed in section 3.3; (2) new artificial random gaps were then created on the gap-filled data sets to test the effect of different locations of missing data while ensuring the reproduction of the exact number and size of each gap for each annual period (for example, the year 2013 had exactly 3 gaps of 1, 6 and 1 consecutive days of missing N_2O fluxes). No artificial gaps were created on previous real gap locations to avoid replacement of a former gap-filled location by the same value; (3) afterwards, gap-filling was again applied to the N_2O flux dataset containing the new gaps; (4) this operation was repeated 100 times on the whole period and allowed 100 annual N_2O budgets to be calculated for each year. The standard deviations calculated over the 100 repetitions indicated the uncertainty related to the gap-filling on each annual N_2O budget.

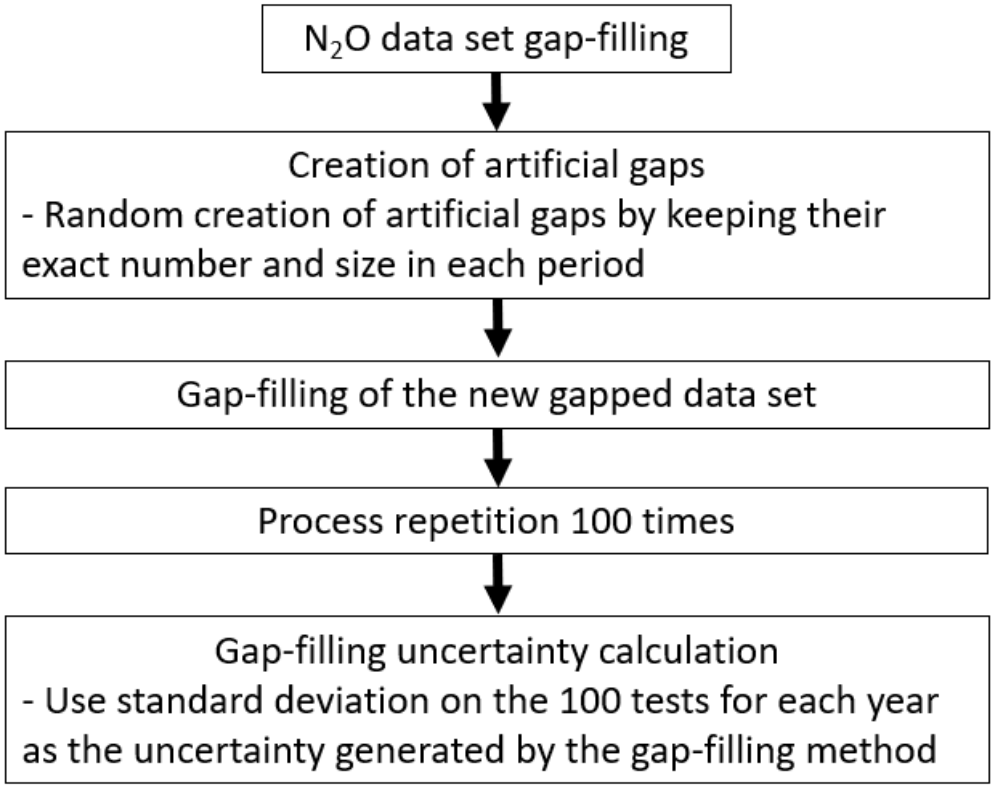

Fig. 6. Diagram outlining the successive steps to calculate the uncertainty due to gap-filing methodology.

344

345 **4. Results and Discussion**

346 *4.1 N_2O flux range and dynamic at FR-Lam crop site*

347 Over the five years of monitoring, the magnitude and timing of measured N_2O fluxes varied
348 according to the soil occupation, the agricultural practices and the climatic year (Fig. 8). Typical
349 variability of N_2O fluxes occurred according to rain, irrigation and fertilisation events. Wheat,
350 cover crops and bare soil periods emitted less N_2O, on average (from 6.6 to 13.0 gN ha^{-1} d^{-1}),
351 than the maize periods (16.3 to 42.9 gN ha^{-1} d^{-1}) (Table 2). Intensity of N_2O fluxes was also
352 higher in the maize periods than in the others, with maximum values ranging between 160 and
353 399, compared to 33 and 133 gN ha^{-1} d^{-1} (Table 2, Fig. 8). Maximum fluxes measured on maize
354 2012 (174 gN ha^{-1} d^{-1}), maize 2015 (160 gN ha^{-1} d^{-1}) and wheat 2013 (33 gN ha^{-1} d^{-1}) were in the

range of those given for wheat – irrigated maize crop rotations in Dhadli et al. (2016) for northern India on a loamy sand soil site (143 and 50 gN ha^{-1} d^{-1} for maize and wheat respectively) and in Han et al. (2016) for northern China (96 and 50 gN ha^{-1} d^{-1} for maize and wheat respectively). Maximum fluxes measured on wheat 2016 (100 gN ha^{-1} d^{-1}) and maize 2014 (399 gN ha^{-1} d^{-1}) were significantly above those generally reported in the literature. Taki et al. (2018) nevertheless measured a maximum N_2O flux of 225 gN ha^{-1} d^{-1} on a maize crop, which is still half that of maize 2014 in this study. The strong N_2O flux peak observed at the end of June 2014 could be explained by optimal conditions for N_2O production: the field operations during that period resulted in easily available N substrate, with two considerable mineral fertilization of 102 and 72 kgN ha^{-1} applied at an interval of only one week, and high soil water content, with two irrigation events one week after N application. We can assume that N_2O fluxes on our site were within the average range of other wheat-maize crop rotation sites but atypical management practices or climate may have led to temporally unusual and important N_2O fluxes.

The bare soil and wheat 2013 periods were the ones with the most and the least missing data, 21% and 1% respectively. The number of consecutive missing daily N_2O fluxes varied from 1 to 62, with a minimum of 1 to 2 on wheat 2013 and a maximum of 1 to 62 on bare soil periods (Table 2). These gaps were due to the removal of chambers for field operations or disturbance of the aero-dynamic conditions, leading to a filtering of the data.

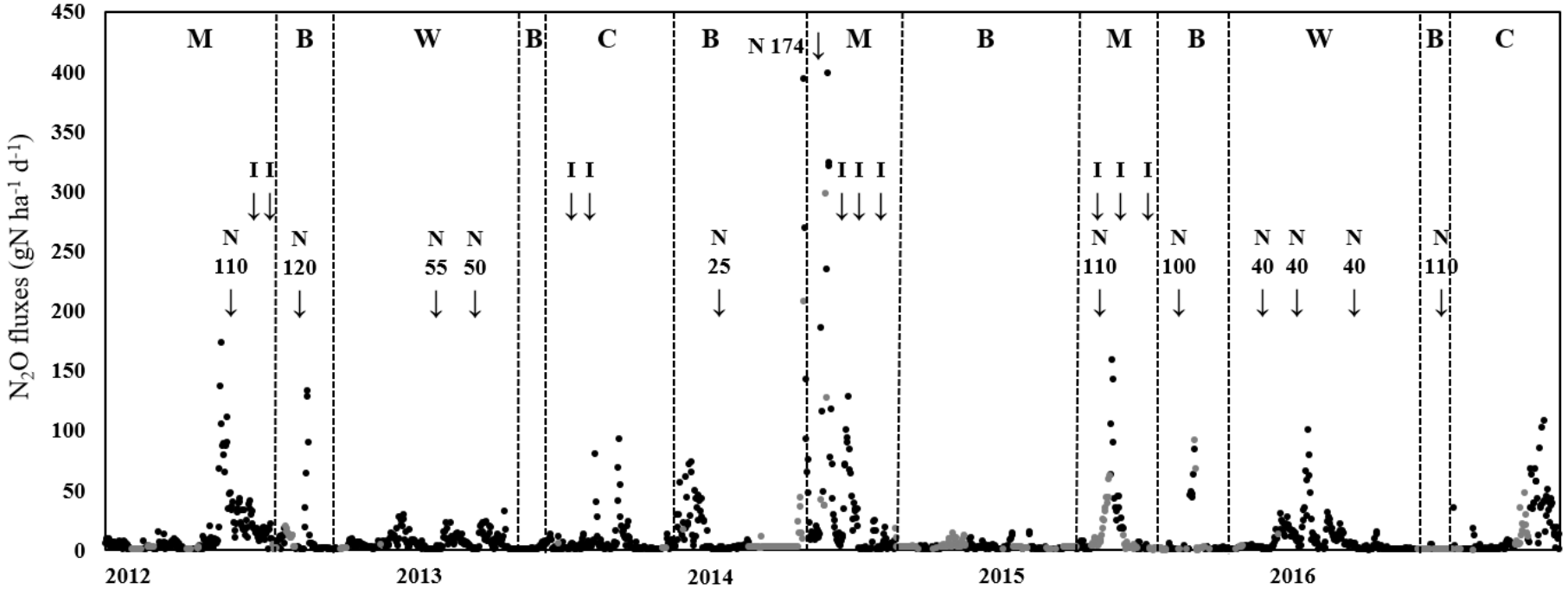

Fig. 7. Daily N_2O fluxes dynamic observed (cross) and gap-filled (dot) at FR-Lam from 2012 to 2016. M: maize; B: bare soil; W: wheat; C: cover crop; N: nitrogen application (kgN ha^{-1}); I: irrigation.

374

375

Vegetation periods	Mean daily N_2O flux (gN ha^{-1} d^{-1})	Maximum daily N_2O flux (gN ha^{-1} d^{-1})	Period length (days)	Number of daily N_2O fluxes missing	Length of consecutive missing daily N_2O fluxes
Maize 2012	25.6 (± 30.0)	174	119	15 (13%)	1 - 10
Maize 2014	42.9 (± 67.0)	399	124	14 (11%)	1 - 7
Maize 2015	16.3 (± 36.2)	160	127	63 (50%)	17 - 25
Wheat 2013	6.6 (± 6.4)	33	257	3 (1%)	1 - 2
Wheat 2016	7.9 (± 16.7)	100	254	7 (3%)	1 - 5
CC 2013	9.3 (± 18.1)	93	90	6 (7%)	6
CC 2016	13.0 (± 22.8)	109	118	25 (21%)	1 - 17
Bare soil periods	7.5 (± 20.7)	133	738	252 (34%)	1 – 62
Lamasquère 2012-2016	12.3 (± 28.8)	399	1 827	385 (21%)	1 - 62

Table 2. Description of the daily N_2O flux dataset at FR-Lam per functioning period.

4.2 ANN simulation and selected variables

The selected input variables varied among the study periods (Table 3). Whatever the combination, all input variables selected for gap-filling (Table 3) had a direct or indirect influence on N_2O emissions (Robertson et al., 1989). Fig. 8 illustrates connections between input variables and the direct proximal factors of denitrification regulation (inspired from Robertson et al., 1989).

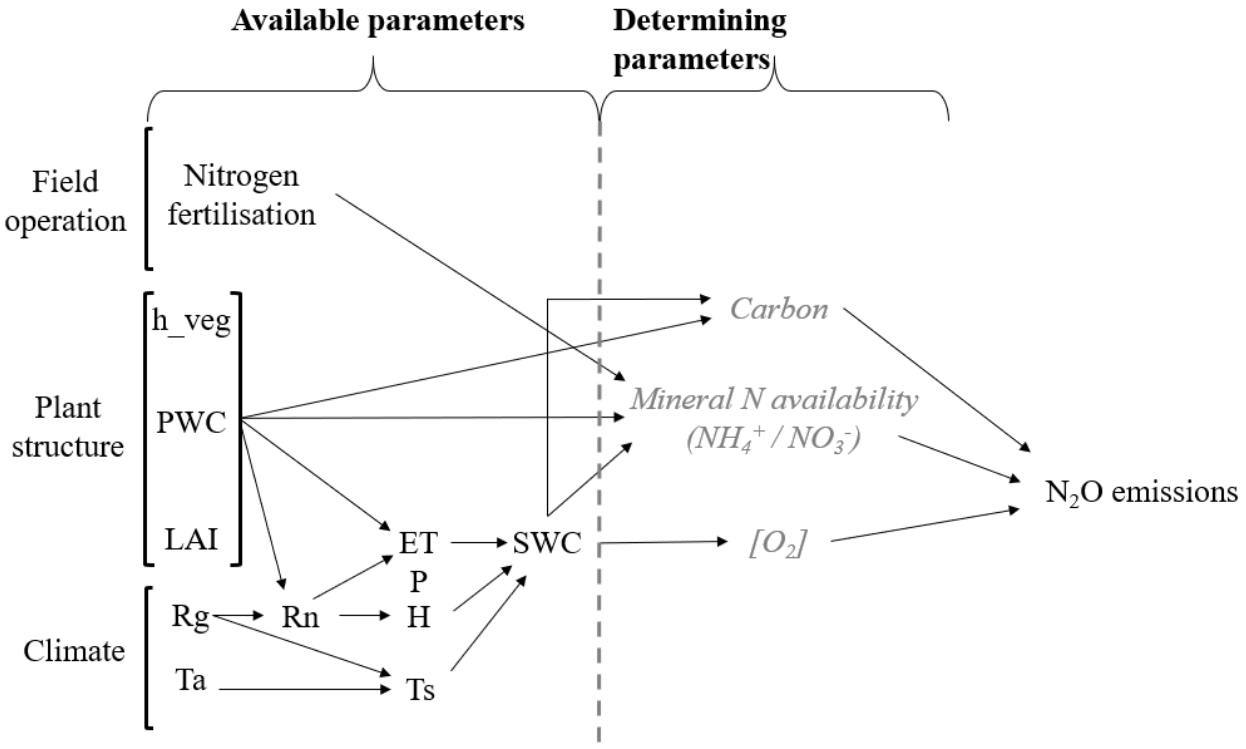

Fig. 8. Illustration of the possible interactions between selected variables and proximal factors of N_2O emissions. Variables in grey italics were not measured or not available.

Variables related to vegetation structure make the greatest contribution to modulating proximal factors and thus to N_2O emission modulation. LAI and h_veg are naturally related to the soil mineral nitrogen availability. These also modulate and reflect the soil dioxygen content via root respiration, the soil water content via potential evapotranspiration (ETP) and the soil carbon content via rhizodeposition and physical disruption by the roots, etc. Net radiation (Rn) corresponds to the available radiative energy in the top of soil – top of canopy continuum, which naturally depends on Rg but also on the crop coverage and structure, and it potentially modulates the heat fluxes that are implicated in soil water loss and soil heating. Sensible heat flux (H) may be linked to soil temperature as an increasing H is associated with surface heating coming from water stress. Finally, the fertilization parameter uses the function established in Eq. 1. to

represent nitrogen application in the field. Taki et al. (2018) partly used the same parameters in all their single-year ANNs, together with air temperature, soil temperature, soil water content, NO_3^- concentration, NH_4^+ concentration with snow depth, rainfall, the season and the time of the year. In contrast with Ryan et al. (2004) and Taki et al. (2018) who both used rainfall as controlling factor, waterfall (rain and irrigation), even tested in applying a lagtime from 0 to 5 days, did not appear to be a significant input parameter in the ANN constructions at FR-Lam. SWC at 50 cm depth appeared more explanatory than rainfall. Moreover, since the water table rose frequently near the soil surface at FR-Lam, SWC at 50 cm parameter reflects environmental conditions' variation related to sub-ground phenomenon on that site in addition to being integrative of the rainfall/irrigation amount. The season and the time of the year were not necessary parameters, as we separated our dataset according to the functioning period, and snow depth was not useful as no significant snowfall occurred during the monitoring. NO_3^- and NH_4^+ concentrations would have been valuable as determining parameters in the formation of N_2O (Fig. 8) but they were not continuously monitored.

An ANN using LAI, Ta_mean, Rn, ETP and SWC_50 as input variables was first tested for the whole period from 2012 to 2016 and led to poor statistical scores with an R^2 of 0.28, an RMSE of 23 gN ha^{-1} d^{-1} and an RRMSE of 189%. We thus separated the data set according to the functioning periods (Table 3) to create a neural network specific to each crop growing season period and a single one combining all bare soil periods with the most explanatory variables. The combination of variables giving the best estimation of N_2O emissions varied from one period to another (Table 3).

Growing season	Variables used to develop ANNs
Maize 2012	LAI, Ta_mean, Rn, ETP, SWC_50
Maize 2014	LAI, Ta_mean, Rn, ETP, SWC_50
Maize 2015	LAI, Rn, ETP, SWC_50, H
Wheat 2013	Fertilization, Ts_50, PWC, h_veg, H
Wheat 2016	Fertilization, Ta_mean, Rn, H, h_veg
CC 2013	Ta_mean, Rn, PWC, h_veg
CC 2016	Ts_50, Rn, SWC_50, h_veg, ETP
Bare soil periods	Ta_mean, Rg, ETP, Fertilization

Table 3 Summary of the selected variables used to develop the different neuronal network at FR-Lam.

4.3. ANN performances

Creating ANNs relating to each functioning period proved to be relevant, with R^2, RMSE and RRMSE ranging from 0.54 to 0.94, from 4.0 to 33.9 gN ha^{-1} d^{-1} and from 62 to 115, respectively (Table 4), far better than the single ANN over the whole period. The R^2 scores are highly improved compared to those of Taki et al. (2018) who found on average R^2 values ranging from 0.19 to 0.65, depending on the cropping year. Two main reasons can explain that important improvement. First, in our study, an ANN model was built specifically for each functioning period and by discriminating bare soil from growing season periods, whereas Taki et al. (2018) built ANN model without discriminating functioning periods. Even if discriminating functioning period makes more difficult the genericity of the ANN algorithm, it is in favour of improving the fineness of the gap-filling. Then, Taki et al. (2018) used scores and results averaged over 44

scenarios for each cropping year whereas in our study, only the best ANN model was kept from the 40 random draws for each studied period and shown here.

Considerable disparity occurred on statistical results according to the functioning period (Table 4). The RRMSE appeared to be high when looking at all functioning periods together and highlighted the fact that the RMSE was of the same magnitude as the average N_2O fluxes in average. With R^2 ranging from 0.85 to 0.94, periods with maize or cover crop showed better performance than periods with wheat or bare soil, showing an R^2 ranging from 0.54 to 0.66. Even though wheat 2016 and bare soils had an RMSE of the same order of magnitude as the other periods, the difference between the observations and the test simulations turned out to be significant during these two periods when related to the average N_2O fluxes with the highest RRMSE values, 115 and 114 % respectively. Wheat and bare soil periods also corresponded to the lowest mean daily N_2O fluxes: 6.6 – 7.5 gN ha^{-1} d^{-1} against 9.3 – 42.0 gN ha^{-1} d^{-1} during maize/cover crop periods (Table 2). These results show that the ANN method would simulate fluxes with high intensity variation, as observed in maize crops, better than fluxes with low intensity variation as observed in winter wheat. However, these scores are close to those reported in the literature for CO_2 flux gap-filling on a forest site (Melesse and Hanley, 2005; Moffat et al., 2007). Accordingly, ANN performances for N_2O flux estimation proved to be relevant even without any diurnal cycle when compared to other CO_2 flux modelling studies.

Growing season	Methodology	R^2	RMSE (gN ha^{-1} d^{-1})	RRMSE (%)
Maize 2012	ANN	0.86	10.8	43
	Linear interpolation	0.85	12.2	49
	Linear interpolation and ANN combine	0.87	10.6	43
Maize 2014	ANN	0.85	33.9	73
	Linear interpolation	0.58	55.6	119
	Linear interpolation and ANN combine	0.85	34.6	74
Maize 2015	ANN	0.94	13.8	82
	Linear interpolation	0.93	14.3	79
	Linear interpolation and ANN combine	0.97	13.4	77
Wheat 2013	ANN	0.54	4.0	65
	Linear interpolation	0.66	3.6	59
	Linear interpolation and ANN combine	0.67	3.5	57
Wheat 2016	ANN	0.60	8.8	115
	Linear interpolation	0.79	6.6	86
	Linear interpolation and ANN combine	0.69	7.8	102
CC 2013	ANN	0.93	4.0	62
	Linear interpolation	0.53	9.2	145
	Linear interpolation and ANN combine	0.93	4.0	62
CC 2016	ANN	0.86	10.0	76
	Linear interpolation	0.64	14.7	111
	Linear interpolation and ANN combine	0.85	10.1	77
Bare soil periods	ANN	0.66	8.6	114
	Linear interpolation	0.76	7.3	96
	Linear interpolation and ANN combine	0.68	8.6	113
All functioning periods together	ANN	0.84	12.4	101
	Linear interpolation	0.68	17.4	141
	Linear interpolation and ANN combine	0.84	12.4	100

455

456

457 *4.4 Evaluation of ANN and linear interpolation methodologies gap-filling performances*

458 Considering all functioning periods together, ANN methodology gave better statistical scores
459 (see Table 4) than the linear interpolation with higher R^2 (0.84 *vs* 0.68) and lower RMSE (12.4 *vs*
460 17.4 gN ha^{-1} d^{-1}) and RRMSE (101 *vs* 141 %). In the same trend, Taki et al. (2018) obtained
461 better statistical scores for the ANN methodology than with the linear interpolation methodology,
462 finding an average R^2 of 0.41 and 0.34 respectively.

Table 4. R^2 and RMSE calculated on testing dataset for ANN, linear interpolation and both methodologies combined for each functioning period.

463 Even if the linear interpolation might give comparable scores, i.e. for maize in 2012 and
464 2015, it proved to perform better when the averaged N_2O fluxes were the lowest, i. e. wheat
465 2013, wheat 2016 and bare soil periods.
466
467 *4.5 Effect of gap-filling methodologies on mean N_2O emissions according to functioning period*
468 To analyse the effects of the two different gap-filling methodologies on the mean N_2O fluxes
469 per period, we applied them separately to gap-fill the real gaps from the studied data set from
470 2012 to 2016. In the case of the ANN methodology, there are no significant differences on the
471 means and standard deviations of the N_2O fluxes before and after gap-filling whatever the period
472 considered, which shows no large N_2O flux variability was created after gap-filling (Table 5). In
473 contrast, large variability appears after gap-filling when the linear interpolation method is used
474 during maize 2014 and bare soil periods : the mean N_2O flux for the maize 2014 period before
475 gap-filling is 42.9 ± 77.7 gN ha^{-1} d^{-1} and becomes 64.5 ± 107.2 gN ha^{-1} d^{-1} after gap-filling; for
476 the bare soil periods, the mean and standard deviations are 7.5 ± 15.0 gN ha^{-1} d^{-1} before gap-
477 filling and 21.3 ± 58.0 gN ha^{-1} d^{-1} after gap-filling. In both cases, the linear interpolation
478 methodology tends to increase mean N_2O fluxes. Based on these results, it appears that either the
479 ANN underestimates, or the linear interpolation overestimates N_2O fluxes, or both are wrong.
480 However, it questions the use of one methodology or the other. To explain these strong
481 differences between the two methodologies, we analysed these specific periods in greater detail.
482

Vegetation periods	Before gap-filling	Gap-filling with ANN	Gap-filling with linear interpolation	Gap-filling with combine methodologies
Maize 2012	25.6 (± 29.9)	24.0 (± 28.2)	23.4 (± 28.5)	23.7 (± 28.4)
Maize 2014	42.9 (± 77.7)	45.5 (± 78.7)	64.5 (± 107.2)	45.5 (± 78.7)
Maize 2015	16.3 (± 32.2)	12.8 (± 25.1)	15.8 (± 25.9)	12.8 (± 25.1)
Wheat 2013	6.6 (± 6.3)	6.6 (± 6.3)	6.5 (± 6.3)	6.5 (± 6.3)
Wheat 2016	7.9 (± 12.5)	7.8 (± 12.4)	7.8 (± 12.4)	7.8 (± 12.4)
CC 2013	9.3 (± 17.2)	8.8 (± 16.7)	9.0 (± 16.6)	8.8 (± 16.7)
CC 2016	13.0 (± 23.4)	13.1 (± 21.5)	10.9 (± 20.8)	12.6 (± 21.5)
Bare soil periods	7.5 (± 15.0)	6.3 (± 13.0)	21.3 (± 58.0)	6.1 (± 13.0)

Table 5. Effect of ANN and linear interpolation gap-filling methodologies on mean N_2O emissions (gN ha^{-1} d^{-1}).

In some specific case, applying a linear interpolation gap-filling on the bare soil periods would introduce an unrealistic continuity such like the period from 06. March 2014 to 19. May 2014 as shown in Fig. 9 (since maize 2014 begins on the 20. May and would have been gap-filled with ANN methodology). It could be explained by the presence of a very long gap of 69 days (from 19. March to 26. May 2014) surrounded by two periods with high N_2O flux amplitudes: 6.7 gN ha^{-1} d^{-1} on 18. March 2014 and 394.6 gN ha^{-1} d^{-1} on 27. May 2014. The linear interpolation dynamics is clearly not suitable during this period. Even if the ANN gap-filling can be wrong, it is more consistent with the dynamics of the observations, in particular since ANN takes the environmental conditions into account, especially since environmental conditions (data not

shown) were not in favour of N_2O production: only 75 mm of rain in 67 days, where the ANN simulated very low N_2O fluxes.

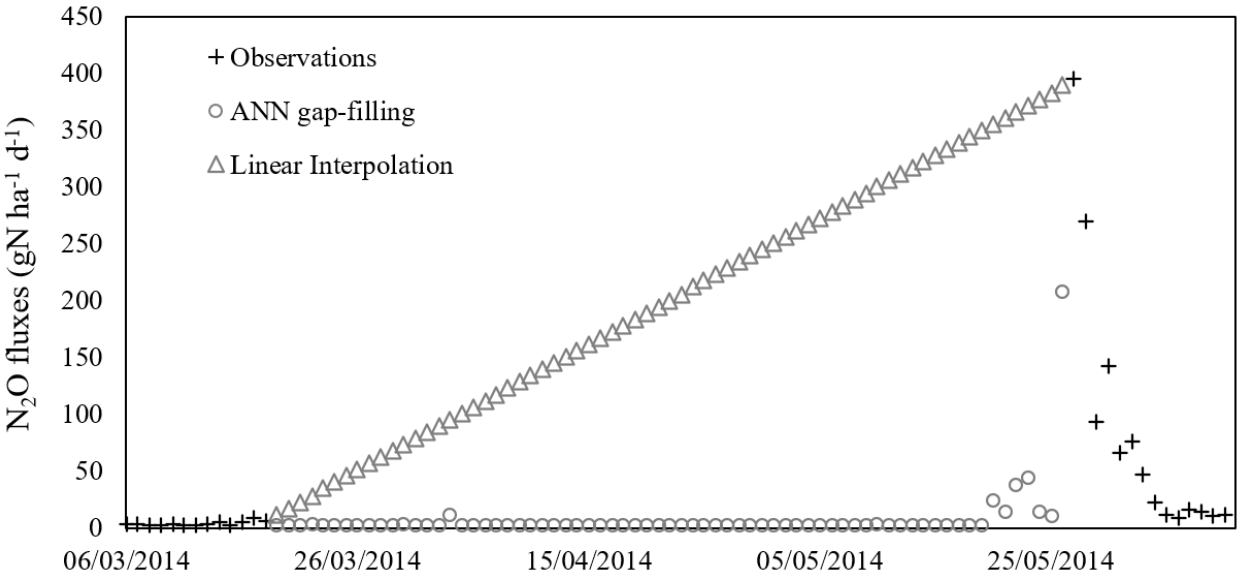

Fig. 9. N_2O fluxes (+) gap-filled by ANN (o) and linear interpolation (Δ) on bare soil period from 05/03/2014 to 19/05/2014 and on maize 2014 period from 20/05/2014 to 09/06/2014.

4.6 Combination of ANN and linear interpolation methodologies

As the linear interpolation method also gives satisfactory statistical results (Table 4), it would have been a loss to set it aside since we have seen that, in some circumstances, this method is better than ANN, especially on periods with low averaged N_2O fluxes. Moreover, in some specific case, like long period of missing data or period with environmental conditions in favour of N_2O emissions, applying a linear interpolation gap-filling could introduce unrealistic N_2O fluxes. In order to fix this, we propose to combine the two gap-filling methodologies depending on the value of GMD ((Eq. 5.), see section 3.3). The RMSE are then compared with GMD values, and used to highlight the potential threshold GMD values on which the selection of the best methodology to gap-fill the data could be based (Table 6).

	Methodology	GMD < 14	14 < GMD < 30	GMD > 30
RMSE (gN ha d^{-1})	Linear interpolation	3.9	11.6	43.7
	ANN	8.8	10.9	27.2

Table 6. RMSE according to gap-filling methodology and GMD coefficient.

Two GMD threshold values were highlighted (Table 6): when GMD < 14, the RMSE of the ANN method was higher than the one from linear interpolation; when 14 < GMD < 30, RMSE were quite similar for both; when GMD > 30, the RMSE of the ANN method was lower than linear interpolation one.

These results suggest that the suitability of a methodology for gap-filling depends on the GMD value. The linear interpolation is preferable when GMD < 14 and the ANN method is preferable when GMD > 30. When 14 < GMD < 30, the use of either interpolation or ANN is possible as both methodologies give approximately the same score. We decided to use the ANN methodology in this case as it allowed capturing the effect of environmental variables on N_2O fluxes. However, in the case of long gaps (when a gap contains more than 15 missing data) bracketed by two low N_2O fluxes with GMD < 14, the decision would be to use the linear interpolation methodology. It would be wise to look at possible important environmental modifications during the gaps, such as heavy rain, irrigation or fertilization events, where it could be more accurate to use the ANN methodology instead.

The combined methodology gave practically the same statistical results over the whole period as those from the ANN methodology with a R^2 and a RMSE of 0.84 and 12.4 gN ha^{-1} d^{-1} for both (Table 4). However, an improvement is seen on the three periods where the linear interpolation

method has better statistical results with the combined methodology compared to the ANN one with a R^2, a RMSE and a RRMSE of 0.68, 8.6 and 113 and of 0.66, 8.6 and 114 respectively for bare soil periods, of 0.69, 7.8 and 102 and of 0.60, 8.8 and 115 respectively for wheat 2016 and of 0.67, 3.5 and 57 and of 0.54, 4.0 and 65 respectively for wheat 2013. These results support the use of a combined methodology instead of applying either the linear interpolation alone or the ANN methodology alone for gap-filling.

4.7 Comparison of the three gap-filling methodologies: linear interpolation, ANN and the combination of both

The simulated N_2O flux dynamic were compared between the three methodologies applied for maize 2014 period (Fig. 10). It showed that the ANN methodology gave on average better statistical scores than the linear interpolation (Table 4) and better reproduced the important peak than did the linear interpolation around the 29 June 2014. However, ANN over estimated low N_2O fluxes measured in early July (Fig. 10 a. and b) where the linear interpolation reproduced much better their low intensity (Fig. 10 b). Although the combined methodology gave approximately the same statistical scores than those of ANN alone (Table 4), it allowed a better catching of N_2O flux dynamic (Fig. 10 c).

In the same way, during periods where the linear interpolation methodology gave better results than the ANN one (Table 4), combining both methodologies helped to better reproduce low fluxes (Fig. 11) and to improve statistical results compared to the ANN with a R^2, a RMSE and a RRMSE of 0.69, 7.8 gN ha^{-1} d^{-1} and 102 for wheat 2016, respectively.

The ANN and the combined methodologies gave on average comparable statistical scores whatever the functioning period probably due to a control by high N_2O flux values. However,

because the combined methodology proved to be more efficient to capture N_2O intensity dynamic it was used to gap-fill missing data from 2012 to 2016 (Fig. 7).

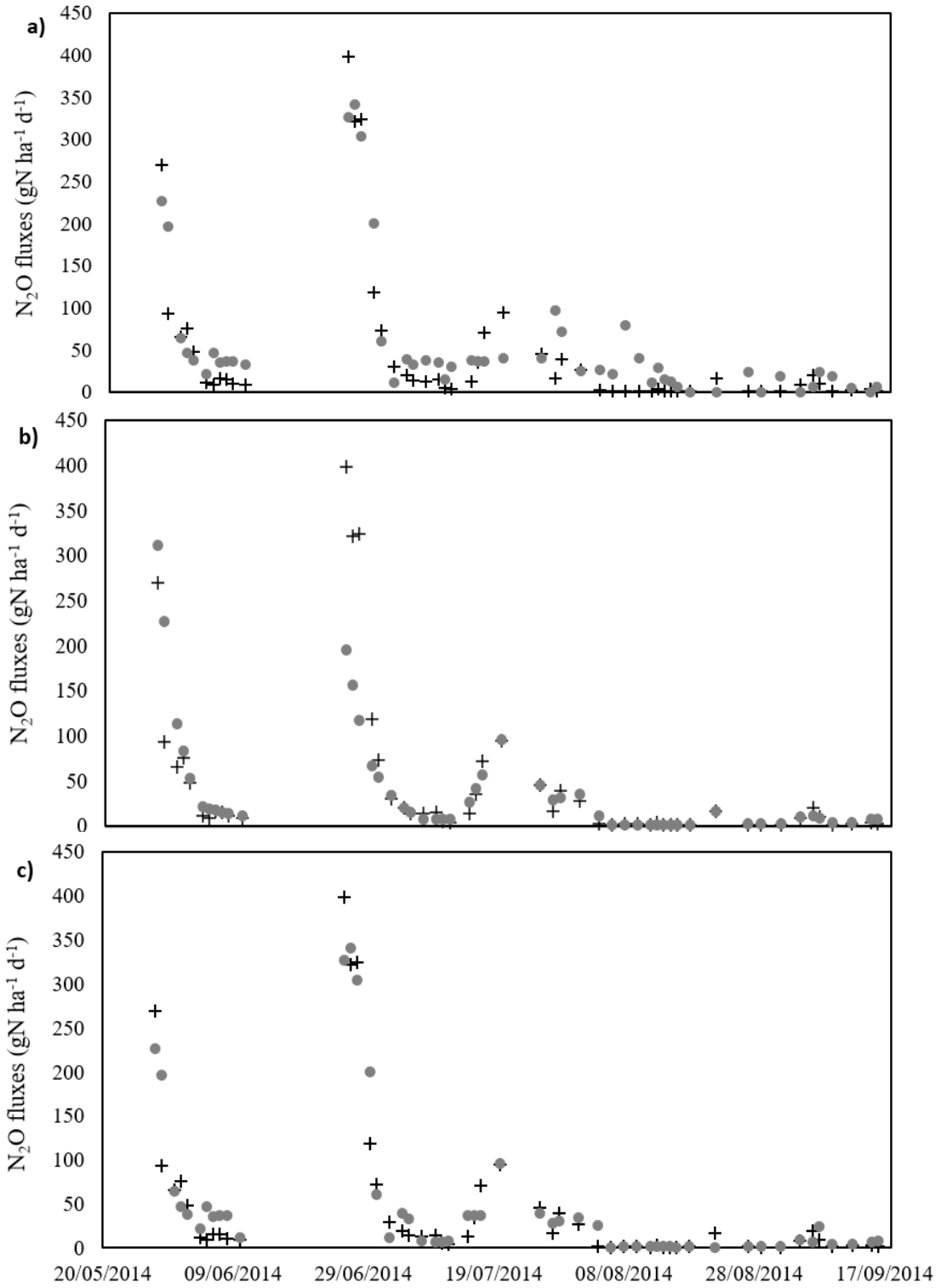

Fig. 10. Comparison between observed (cross) and simulated (dot) N_2O fluxes dynamic according to gap-filling methodology ANN (a), linear interpolation (b) and mixed methodology (c) on Maize 2014. Only the days used for the test dataset are shown here.

553

554

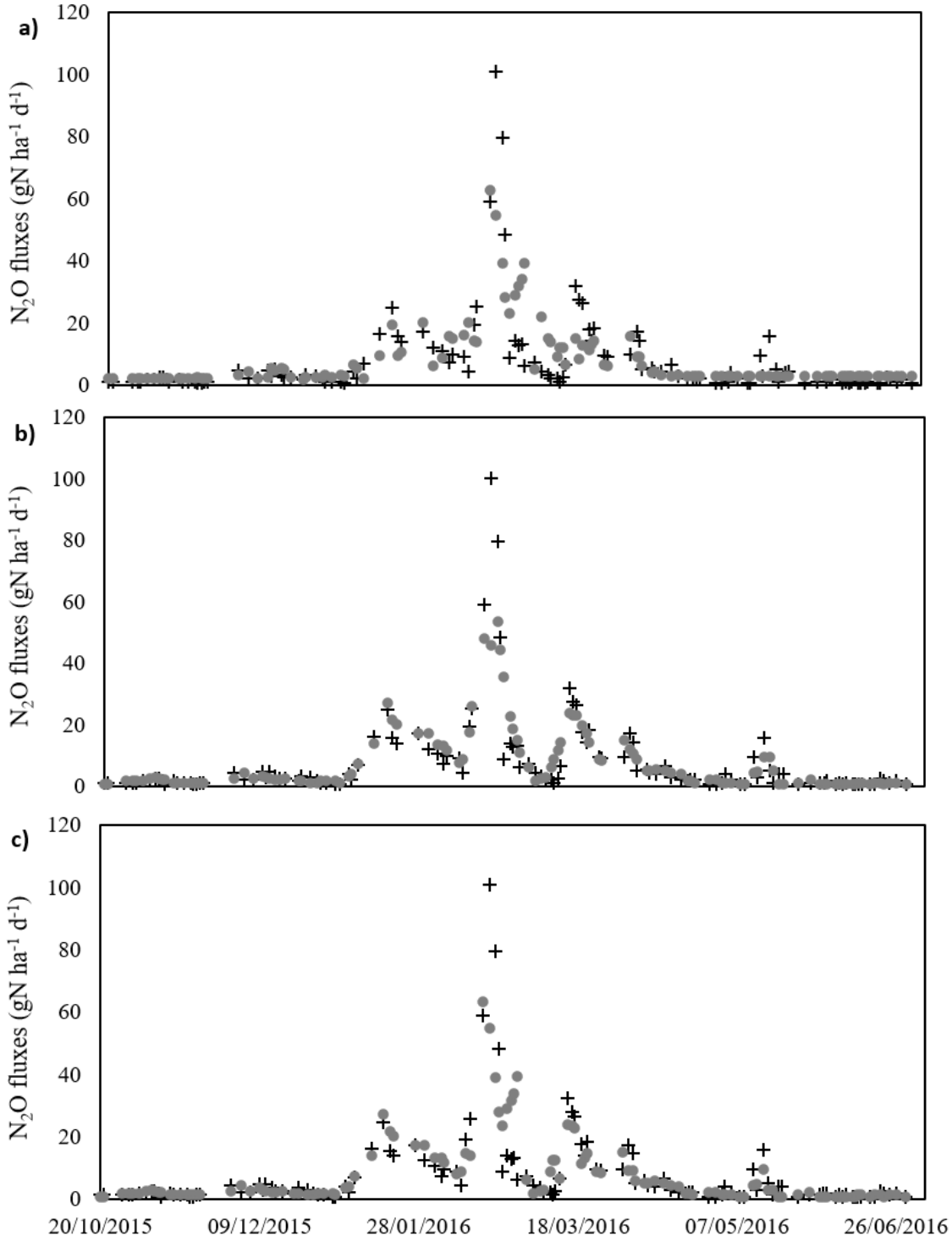

Fig. 11. Comparison between observed (cross) and simulated (dot) N_2O fluxes dynamic according to gap-filling methodology ANN (a), linear interpolation (b) and mixed methodology (c) on Wheat 2016. Only the days used for the test dataset are shown here.

555

5. Evaluation of gap-filling uncertainty on N_2O budget

The uncertainties on the N_2O annual budget related to the gap-filling varied between ± 25 and ± 198 gN ha^{-1} among years, and between 0.9 and 4.1 % when looking at the relative uncertainty (Table 7) calculated via the methodology described in section 3.4. Gap-filling had a particularly low impact on year 2013 (Table 7) as there were only few gaps during this period: 3 gaps with respectively 1, 6 and 1 missing value(s). These results are relatively low compared to the annual uncertainties calculated by Taki et al. (2018), who obtained an uncertainty variation among years of ± 70 to ± 810 gN ha^{-1} and 7 to 24 % when looking at the relative uncertainty using ANN as gap-filling method, and an uncertainty variation among years of ± 40 to ± 470 gN ha^{-1} and 5 to 15 % when looking at the relative uncertainty using linear interpolation as the gap-filling method. These differences with our results could be explained by the different methods adopted. Their results also prove that a combination of both methodologies may improve the gap-filling as their N_2O annual budget uncertainties were lower with the linear interpolation than with the ANN methodology, despite the fact that they found a better R^2 for the ANN. These uncertainty differences among years can be explained by the disparities in the number and size of gaps and in the intensity of N_2O emissions among years: years with a high N_2O budget (related to high N_2O fluxes), especially observed during maize periods, and with a small number of gaps lead to a low gap-filling uncertainty whereas the uncertainty increases when the length of gaps increases and N_2O flux intensity is low, especially for wheat and bare soil periods. Nevertheless, the results show that the proposed mixed gap-filling methodology performs well when used on annual N_2O flux datasets with a relative uncertainty below 5 % for each year.

	Annual N_2O budget after gap-filling ($kgN\ ha^{-1}$)	Sd ($kgN\ ha^{-1}$)	Relative uncertainty (%)	Number of missing values (days)
2012	4.21	0.128	3.0	55
2013	2.75	0.025	0.9	8
2014	7.46	0.198	2.8	137
2015	3.01	0.124	4.1	127
2016	3.59	0.127	3.4	58

Table 7. N_2O budget gap-filling uncertainty per civil year. Mean and standard deviation were calculated using the 100 repetitions.

Conclusion

Three different gap-filling methodologies were examined with respect to their performance for filling gaps in long-term N_2O flux data series. This study has demonstrated that the use of an artificial neural network could be a helpful tool to gap-fill daily N_2O fluxes as already recommended for other greenhouse gases such as CO_2 and CH_4. On average, ANN proved to give better gap-filling performance than linear interpolation when looking at the R^2 and RMSE scores, even though linear interpolation performed better when gap-filling N_2O fluxes of low intensity. Thus, the study proposes a new approach to gap-fill N_2O emissions by combining the advantages of both methodologies. Such a procedure, which is not very costly in computing time and in requested variables (4 to 5 in our case), may be very helpful for future works on N_2O emission analysis, especially on sites where numerous continuous variables are monitored (fluxnet and ICOS sites for example). In particular, it may improve the calculated N_2O budget with limited gap-filling uncertainty, below 5% in this study. Moreover, given the strong non-linearity of N_2O emissions due to multiple interactions between controlling environmental variables, ANN has the advantage of reproducing a complex process without any a priori knowledge of the system, and is

flexible and easy to use. The GMD thresholds developed in this study figures to be site specific as they highly depend on the ANNs performances and thus on quality and number of explanatory variables that may strongly vary among study sites. That saying, as the eddy covariance methodology is becoming more and more used across agricultural sites and for processes studies, besides the fact that higher available dataset could improve the methodology performance, further evaluation of the mixed gap-filling methodology should be carried out for N_2O fluxes measured and compiled at higher resolution than the day (e.g. 6-hourly data).

Acknowledgement

Research for this article was supported by a public grant received from the French Ministry of Higher Education, Research and Innovation. Data acquisition at FR-Lam are mainly funded by the Institut National des Sciences de l'Univers (INSU) through the ICOS and OSR SW observatories. Facilities and staff are funded and supported by the Observatory Midi-Pyrenean, the University Paul Sabatier of Toulouse, CNRS (Centre National de la Recherche Scientifique), CNES (Centre National d'Etude Spatial) and IRD (Institut de Recherche pour le Développement). We are grateful to Franck Granouillac, Nicole Claverie and Bartosz Zawilski for their technical support, advice, and valuable assistance in the field and site management, respectively and Aurore Brut for the data processing. Special thanks to the Ecole Supérieure d'Agriculture de Purpan for accommodating our measurement devices in their field.

References

Béziat, P., et al., 2009. Carbon balance of a three crop succession over two cropland sites in South West France. Agricultural and Forest Meteorology 149, 1628–1645. https://doi.org/10.1016/j.agrformet.2009.05.004

Bishop, C., 1995. Neural Networks for Pattern Recognition. Oxford University Press; New York, USA.

Davidson, E.A., 2009. The contribution of manure and fertilizer nitrogen to atmospheric nitrous oxide since 1860. Nature Geoscience 2, 659–662. https://doi.org/10.1038/ngeo608

Dengel, S., et al., 2013. Testing the applicability of neural networks as a gap-filling method using CH4 flux data from high latitude wetlands. Biogeosciences 10, 8185–8200. https://doi.org/10.5194/bg-10-8185-2013

Delon, C., et al., 2007. Soil NO emissions modelling using artificial neural network. Tellus B: Chemical and Physical Meteorology 59, 502–513. https://doi.org/10.1111/j.1600-0889.2007.00254.x

Dhadli, H.S., et al., 2016. N2O emissions in a long-term soil fertility experiment under maize–wheat cropping system in Northern India. Geoderma Regional 7, 102–109. https://doi.org/10.1016/j.geodrs.2016.02.003

Franz, D., et al., 2018. Towards long-term standardised carbon and greenhouse gas observations for monitoring Europe´s terrestrial ecosystems: a review. Int. Agrophys. 32, 439–455. https://doi.org/10.1515/intag-2017-0039

Gaillardet, J., et al., 2018. OZCAR: The French Network of Critical Zone Observatories. Vadose Zone Journal 17, 0. https://doi.org/10.2136/vzj2018.04.0067

Grossel, A., et al., 2014. Simulating the spatial variability of nitrous oxide emission from cropped soils at the within-field scale using the NOE model. Ecological Modelling 288, 155–165. https://doi.org/10.1016/j.ecolmodel.2014.06.007

Guenther, F., Fritsch, S., 2010. neuralnet: Training of neural networks 2, 9.

Han, X., et al., 2016. Effects of Reduced Nitrogen Fertilization and Biochar Application on CO_2 and N_2O Emissions from a Summer Maize-Winter wheat Rotation Field in North China. Agricultural Science & Technology, 2016, 17(12): 2800-2808.

Hénault, C., et al., 2005. Predicting in situ soil N2O emission using NOE algorithm and soil database. Global Change Biology 11, 115–127. https://doi.org/10.1111/j.1365-2486.2004.00879.x

Hénault, C., et al., 2012. Nitrous Oxide Emission by Agricultural Soils: A Review of Spatial and Temporal Variability for Mitigation. Pedosphere 22, 426–433. https://doi.org/10.1016/S1002-0160(12)60029-0

Lognoul, M., et al., 2017. Impact of tillage on greenhouse gas emissions by an agricultural crop and dynamics of N2O fluxes: Insights from automated closed chamber measurements. Soil and Tillage Research 167, 80–89. https://doi.org/10.1016/j.still.2016.11.008

IPCC, 2013. Observations: atmosphere and surface. In: Stocker, T.F., et al., 2013. Climate Change 2013: The Physical Science Basis. Contribution of Working Group I to the Fifth Assessment Report of the Intergovernmental Panel on Climate Change. Cambridge University Press, Cambridge, United Kingdom and New York, NY, USA, pp. 167–168.

Knowles, R., 1982. Denitrification. Microbiology and Molecular Biology reviews 46, 43-70

Lek, S., Delacoste, M., Baran, P., Dimopoulos, I., Lauga, J., Aulagnier, S., 1996. Application of neural network for nonlinear modeling in ecology. Ecological Modelling 90, 39–52

Li, C., et al., 2000. A process-oriented model of N2O and NO emissions from forest soils: 1. Model development. J. Geophys. Res. 105, 4369–4384. https://doi.org/10.1029/1999JD900949

Melesse, A.M., Hanley, R.S., 2005. Artificial neural network application for multi-ecosystem carbon flux simulation. Ecological Modelling 189, 305–314. https://doi.org/10.1016/j.ecolmodel.2005.03.014

Moffat, A.M., et al., 2007. Comprehensive comparison of gap-filling techniques for eddy covariance net carbon fluxes. Agricultural and Forest Meteorology 147, 209–232. https://doi.org/10.1016/j.agrformet.2007.08.011

Nemitz, E., et al., 2018. Standardisation of eddy-covariance flux measurements of methane and nitrous oxide. International Agrophysics 32, 517–549. https://doi.org/10.1515/intag-2017-0042

Olden, J.D., Jackson D.A., 2002. Illuminating the ‘‘black box’’: a randomization approach for understanding variable contributions in artificial neural networks. Ecological Modelling 154, 135–150

Papale, D., Valentini, R., 2003. A new assessment of European forests carbon exchanges by eddy fluxes and artificial neural network spatialization. Global Change Biology 9, 525–535. https://doi.org/10.1046/j.1365-2486.2003.00609.x

Parsons, W.F.J., et al., 1993. Nitrate limitation of N2O production and denitrification from tropical pasture and rain forest soils. Biogeochemistry 22, 179–193. https://doi.org/10.1007/BF00000646

Peyrard, C., et al., 2016. N2O emissions of low input cropping systems as affected by legume and cover crops use. Agriculture, Ecosystems & Environment 224, 145–156. https://doi.org/10.1016/j.agee.2016.03.028

Prosser, JI., 1986. Nitrification. IRL Press, Oxford
Ravishankara, A.R., et al., 2009. Nitrous Oxide (N2O): The Dominant Ozone-Depleting Substance Emitted in the 21st Century. Science 326, 123–125. https://doi.org/10.1126/science.1176985
Reeves, S., Wang, W., 2015. Optimum sampling time and frequency for measuring N2O emissions from a rain-fed cereal cropping system. Science of The Total Environment 530–531, 219–226. https://doi.org/10.1016/j.scitotenv.2015.05.117
Reeves, S., et al., 2016. Quantifying nitrous oxide emissions from sugarcane cropping systems: Optimum sampling time and frequency. Atmospheric Environment 136, 123–133. https://doi.org/10.1016/j.atmosenv.2016.04.008
Richardson, A.D., Hollinger, D.Y., 2007. A method to estimate the additional uncertainty in gap-filled NEE resulting from long gaps in the CO2 flux record. Agricultural and Forest Meteorology 147, 199–208. https://doi.org/10.1016/j.agrformet.2007.06.004
Robertson, G. P. 1989. Nitrification and denitrification in humid tropical ecosystems: potential controls on nitrogen retention. Pages 55-69 in J. Proctor, editor. Mineral nutrients in tropical forest and savanna ecosystems. Blackwell Scientific, Cambridge, Massachusetts, USA.
Ryan, M., et al., 2004. The use of artificial neural networks (ANNs) to simulate N2O emissions from a temperate grassland ecosystem. Ecological Modelling 175, 189–194. https://doi.org/10.1016/j.ecolmodel.2003.10.010
Schmidt, M., et al., 2012. The carbon budget of a winter wheat field: An eddy covariance analysis of seasonal and inter-annual variability. Agricultural and Forest Meteorology 165, 114–126. https://doi.org/10.1016/j.agrformet.2012.05.012
Snyder, C.S., et al., 2009. Review of greenhouse gas emissions from crop production systems and fertilizer management effects. Agriculture, Ecosystems & Environment, Reactive nitrogen in agroecosystems: Integration with greenhouse gas interactions 133, 247–266. https://doi.org/10.1016/j.agee.2009.04.021
Taki, R., et al., 2018. Comparison of two gap-filling techniques for nitrous oxide fluxes from agricultural soil. Can. J. Soil Sci. dx.doi.org/10.1139/cjss-2018-0041
Tallec, T., et al., 2013. Crops' water use efficiencies in temperate climate: Comparison of stand, ecosystem and agronomical approaches. Agricultural and Forest Meteorology 168, 69–81. https://doi.org/10.1016/j.agrformet.2012.07.008
Tallec, T., et al., 2019. N2O flux measurements over an irrigated maize crop: A comparison of three methods. Agricultural and Forest Meteorology 264, 56–72. https://doi.org/10.1016/j.agrformet.2018.09.017
Tellez-Rio, A., et al., 2015. N2O and CH4 emissions from a fallow–wheat rotation with low N input in conservation and conventional tillage under a Mediterranean agroecosystem. Science of The Total Environment 508, 85–94. https://doi.org/10.1016/j.scitotenv.2014.11.041
UNEP, 2012. Growing greenhouse gas emissions due to meat production.
Ussiri, D., Lal, R., 2013. The Role of Nitrous Oxide on Climate Change, in: Soil Emission of Nitrous Oxide and Its Mitigation. Springer Netherlands, Dordrecht, pp. 1–28. https://doi.org/10.1007/978-94-007-5364-8_1
Villa-Vialaneix, N., et al., 2012. A comparison of eight metamodeling techniques for the simulation of N2O fluxes and N leaching from corn crops. Environmental Modelling & Software, Emulation techniques for the reduction and sensitivity analysis of complex environmental models 34, 51–66. https://doi.org/10.1016/j.envsoft.2011.05.003
Vinzent, B., et al., 2017. Efficacy of agronomic strategies for mitigation of after-harvest N2O emissions of winter oilseed rape. European Journal of Agronomy 89, 88–96. https://doi.org/10.1016/j.eja.2017.06.009
WMO, 2017. The State of Greenhouse Gases in the Atmosphere Based on Global Observations through 2017. WMO Greenhouse gas Bulletin No. 14., Geneva. https://library.wmo.int/doc_num.php?explnum_id=5455
Wijler, J., Delwiche, C.C., 1954. Investigations on the denitrifying process in soil. Plant Soil 5, 155–169. https://doi.org/10.1007/BF01343848
Zhang, Y., et al., 2016. Application of the DNDC model to estimate N2O emissions under different types of irrigation in vineyards in Ningxia, China. Agricultural Water Management 163, 295–304. https://doi.org/10.1016/j.agwat.2015.10.006

table 1.png

Variable names	Variable description (unit)
ABG	Above Ground Biomass (kg m^{-2})
E	Measured Evapotranspiration (kg m^{-2} d^{-1})
ETP	Potential Evapotranspiration (mm)
GPP	Green Primary Production (gC m^{-2} d^{-1})
H	Sensible heat flux (watt m^{-2} d^{-1})
h_veg	Vegetation height (m)
LAI	Leaf Area Index (m^2 m^{-2})
LE	Latent heat flux (W m^{-2} d^{-1})
LW	Incoming long wave (W m^{-2} d^{-1})
NEE	Net Ecosystem Exchange (gC m^{-2} d^{-1})
P	Rain (mm)
Pa	Pressure (kPa)
PPFD	Photosynthetic Photon Flux Density (µmol m^{-2} d^{-1})
PWC	Plant Water Content (%)
Reco	Ecosystem respiration from soil (gC m^{-2} d^{-1})
RH	Relative humidity (%)
Rg	Global radiation (MJ m^{-2} d^{-1})
Rn	Net radiation (W m^{-2} d^{-1})
SWC	Soil Water Content at 0, 5, 10, 30, 50 and 100 cm (%)
Ta_max	Maximum air temperature of the day (°C)
Ta_mean	Mean air temperature of the day (°C)
Ta_min	Minimum air temperature of the day (°C)
Ts	Soil temperature at 0, 5, 10, 30, 50 and 100 cm (°C)
Waterfall	Daily rain and irrigation event (mm)
WS	Wind speed (m s^{-1})

table 3.png

Growing season	Variables used to develop ANNs
Maize 2012	LAI, Ta_mean, Rn, ETP, SWC_50
Maize 2014	LAI, Ta_mean, Rn, ETP, SWC_50
Maize 2015	LAI, Rn, ETP, SWC_50, H
Wheat 2013	Fertilization, Ts_50, PWC, h_veg, H
Wheat 2016	Fertilization, Ta_mean, Rn, H, h_veg
CC 2013	Ta_mean, Rn, PWC, h_veg
CC 2016	Ts_50, Rn, SWC_50, h_veg, ETP
Bare soil periods	Ta_mean, Rg, ETP, Fertilization

table 4.png

Growing season	Methodology	R^2	RMSE (gN ha^{-1} d^{-1})	RRMSE (%)
Maize 2012	ANN	0.86	10.8	43
	Linear interpolation	0.85	12.2	49
	Linear interpolation and ANN combine	0.87	10.6	43
Maize 2014	ANN	0.85	33.9	73
	Linear interpolation	0.58	55.6	119
	Linear interpolation and ANN combine	0.85	34.6	74
Maize 2015	ANN	0.94	13.8	82
	Linear interpolation	0.93	14.3	79
	Linear interpolation and ANN combine	0.97	13.4	77
Wheat 2013	ANN	0.54	4.0	65
	Linear interpolation	0.66	3.6	59
	Linear interpolation and ANN combine	0.67	3.5	57
Wheat 2016	ANN	0.60	8.8	115
	Linear interpolation	0.79	6.6	86
	Linear interpolation and ANN combine	0.69	7.8	102
CC 2013	ANN	0.93	4.0	62
	Linear interpolation	0.53	9.2	145
	Linear interpolation and ANN combine	0.93	4.0	62
CC 2016	ANN	0.86	10.0	76
	Linear interpolation	0.64	14.7	111
	Linear interpolation and ANN combine	0.85	10.1	77
Bare soil periods	ANN	0.66	8.6	114
	Linear interpolation	0.76	7.3	96
	Linear interpolation and ANN combine	0.68	8.6	113
All functioning periods together	ANN	0.84	12.4	101
	Linear interpolation	0.68	17.4	141
	Linear interpolation and ANN combine	0.84	12.4	100

table 5.png

Vegetation periods	Before gap-filling	Gap-filling with ANN	Gap-filling with linear interpolation	Gap-filling with combine methodologies
Maize 2012	25.6 (± 29.9)	24.0 (± 28.2)	23.4 (± 28.5)	23.7 (± 28.4)
Maize 2014	42.9 (± 77.7)	45.5 (± 78.7)	64.5 (± 107.2)	45.5 (± 78.7)
Maize 2015	16.3 (± 32.2)	12.8 (± 25.1)	15.8 (± 25.9)	12.8 (± 25.1)
Wheat 2013	6.6 (± 6.3)	6.6 (± 6.3)	6.5 (± 6.3)	6.5 (± 6.3)
Wheat 2016	7.9 (± 12.5)	7.8 (± 12.4)	7.8 (± 12.4)	7.8 (± 12.4)
CC 2013	9.3 (± 17.2)	8.8 (± 16.7)	9.0 (± 16.6)	8.8 (± 16.7)
CC 2016	13.0 (± 23.4)	13.1 (± 21.5)	10.9 (± 20.8)	12.6 (± 21.5)
Bare soil periods	7.5 (± 15.0)	6.3 (± 13.0)	21.3 (± 58.0)	6.1 (± 13.0)

table 6.png

	Methodology	GMD < 14	14 < GMD < 30	GMD > 30
RMSE (gN ha d^{-1})	**Linear interpolation**	3.9	11.6	43.7
	ANN	8.8	10.9	27.2

table 7.png

	Annual N_2O budget after gap-filling (kgN ha^{-1})	Sd (kgN ha^{-1})	Relative uncertainty (%)	Number of missing values (days)
2012	4.21	0.128	3.0	55
2013	2.75	0.025	0.9	8
2014	7.46	0.198	2.8	137
2015	3.01	0.124	4.1	127
2016	3.59	0.127	3.4	58

fig. 1.png

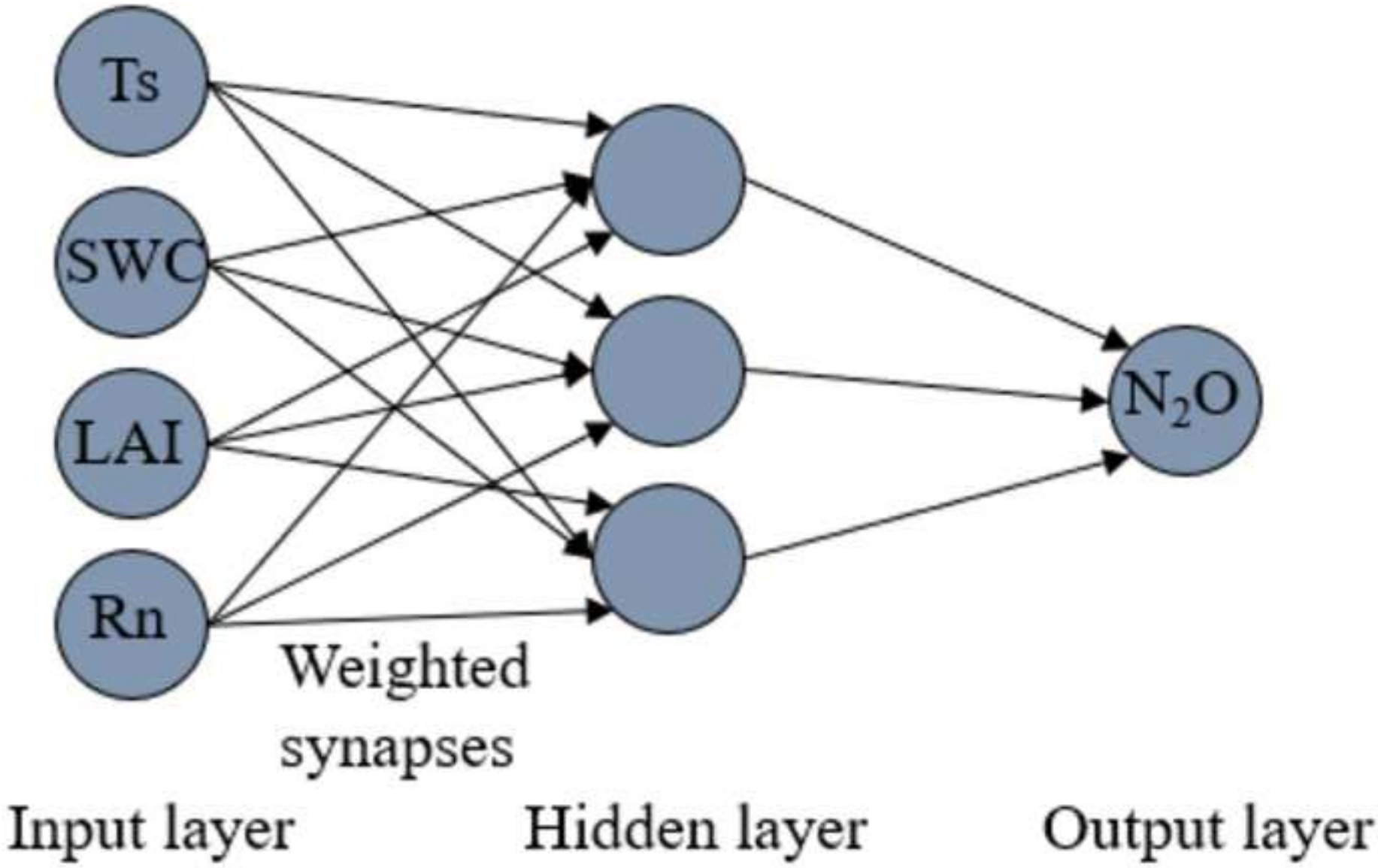
Ts
SWC
LAI
Rn
N_2O
Weighted synapses
Input layer
Hidden layer
Output layer

fig. 10. a.png

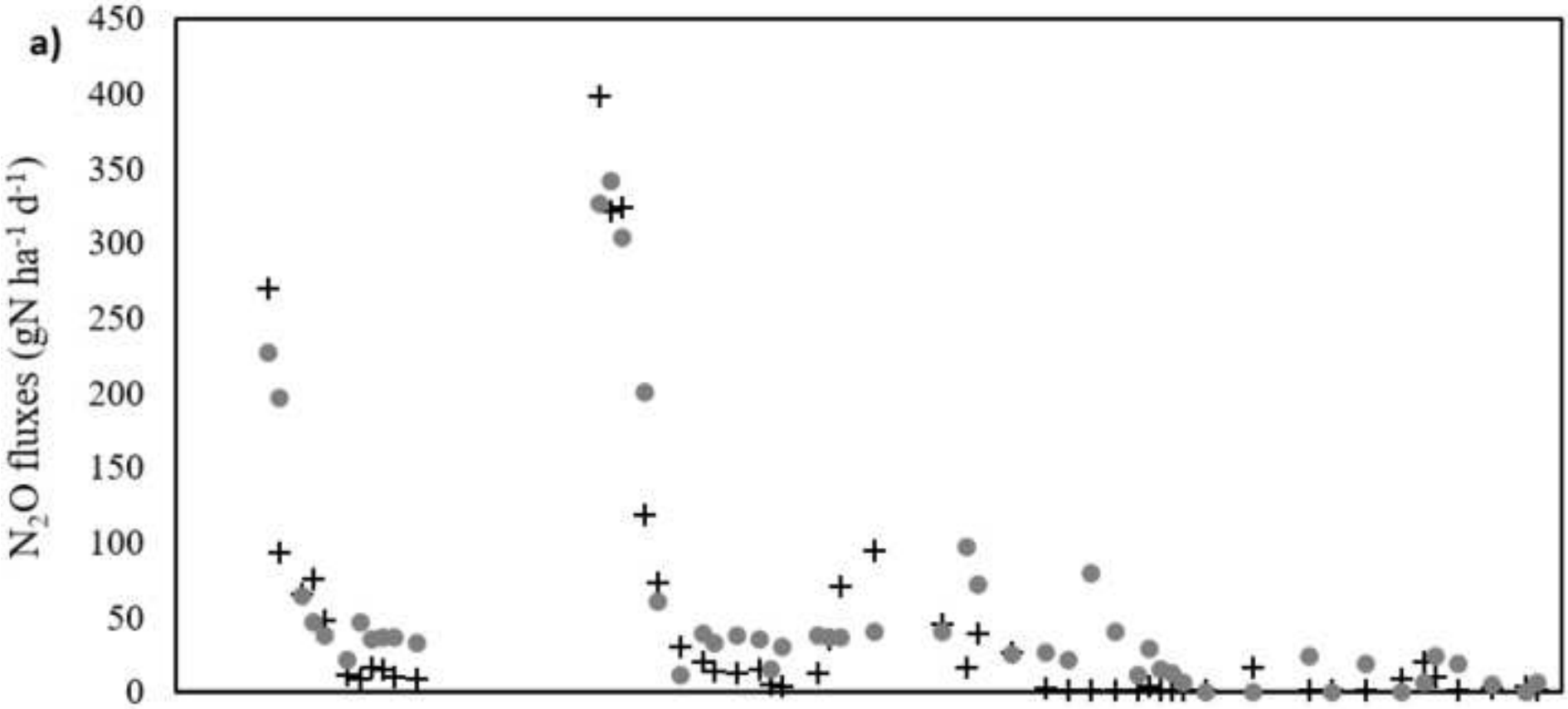

fig. 10. b.png

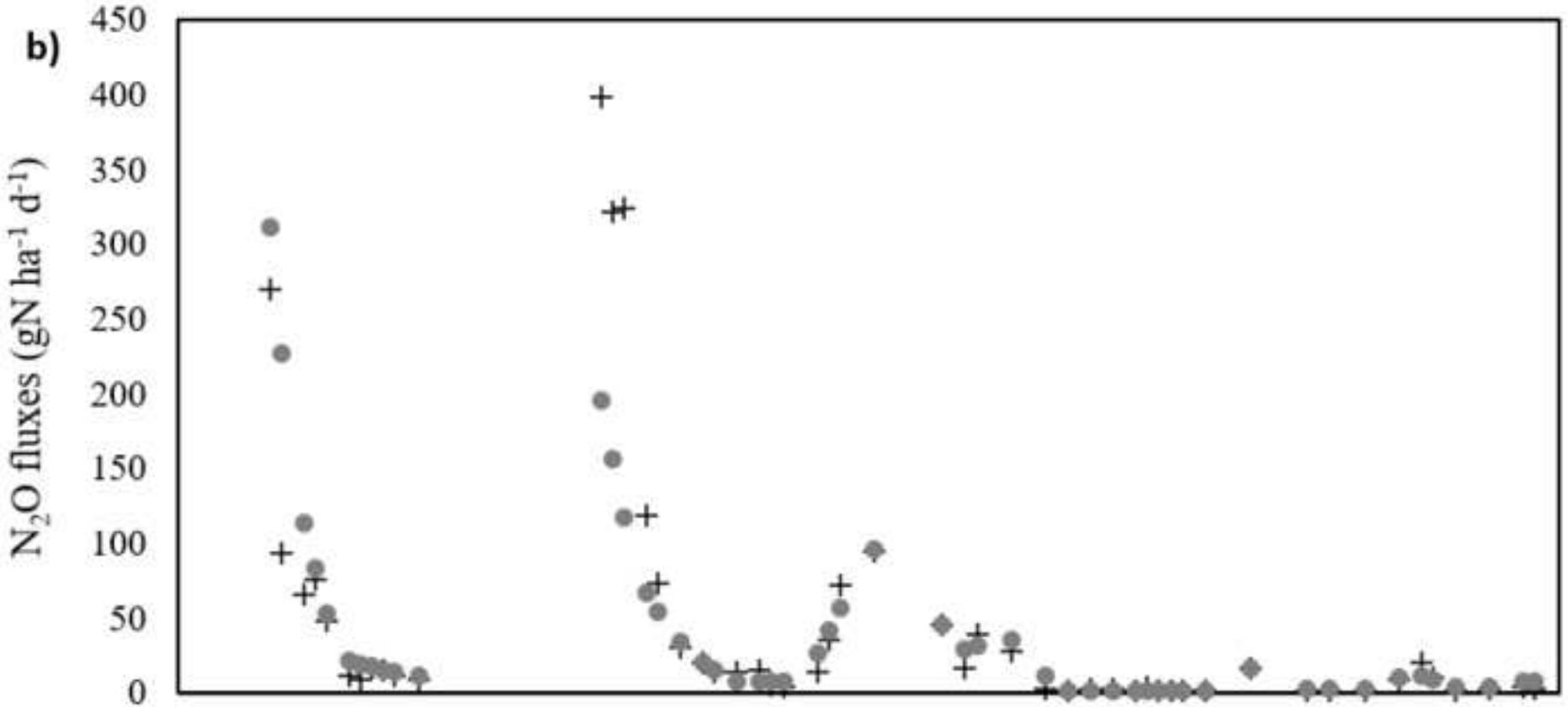

fig. 10. c.png

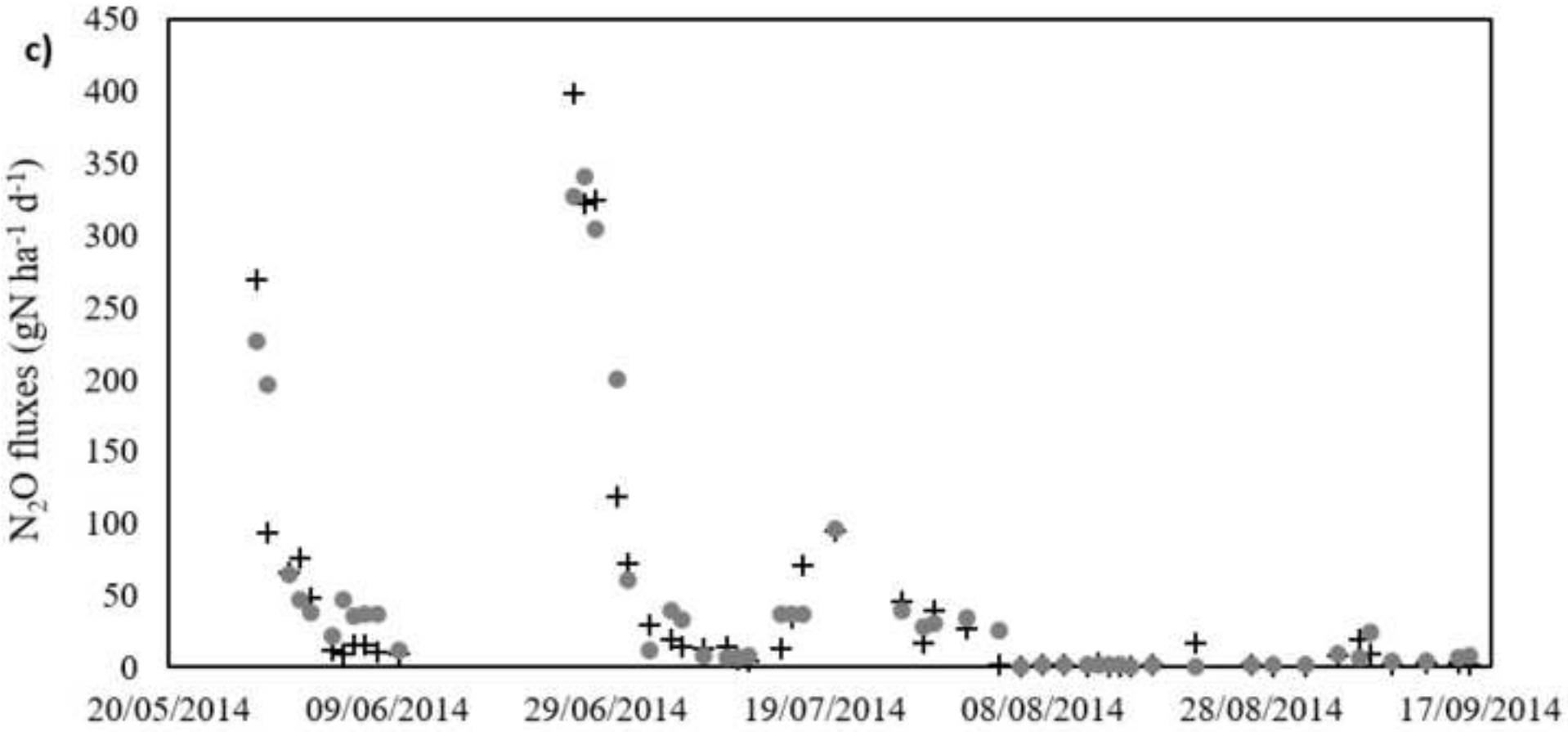
c)
450
400
350
300
250
200
150
100
50
0
N2O fluxes (gN ha-1 d-1)
20/05/2014
09/06/2014
29/06/2014
19/07/2014
08/08/2014
28/08/2014
17/09/2014

fig. 11. a.png

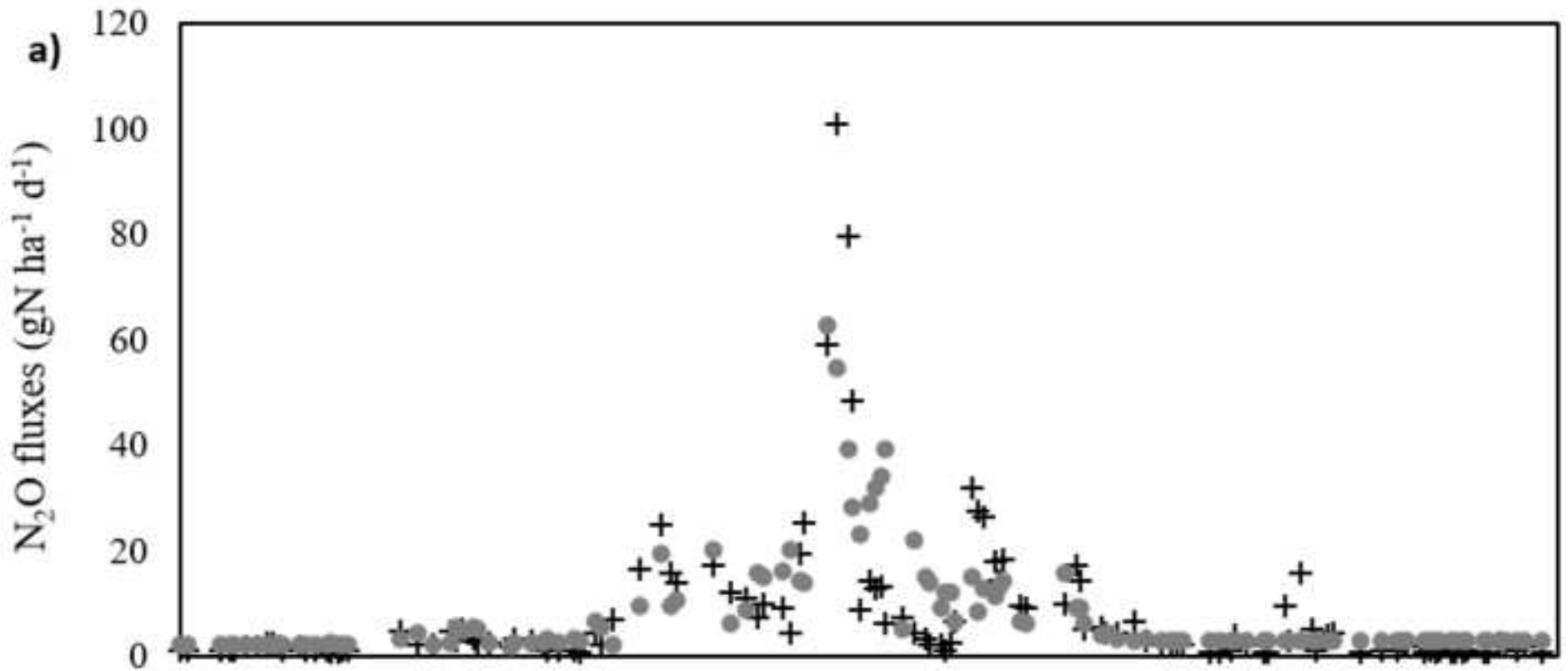

fig. 11. b.png

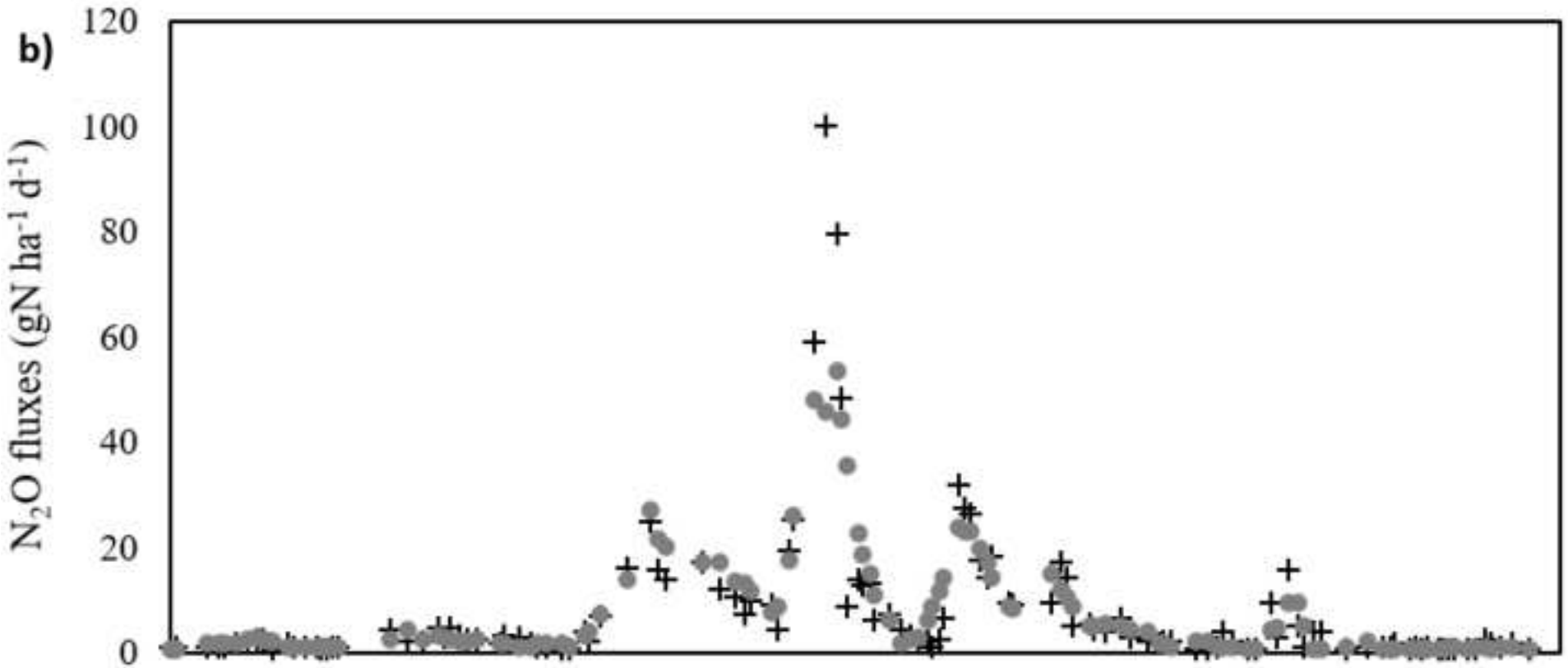

fig. 11. c.png

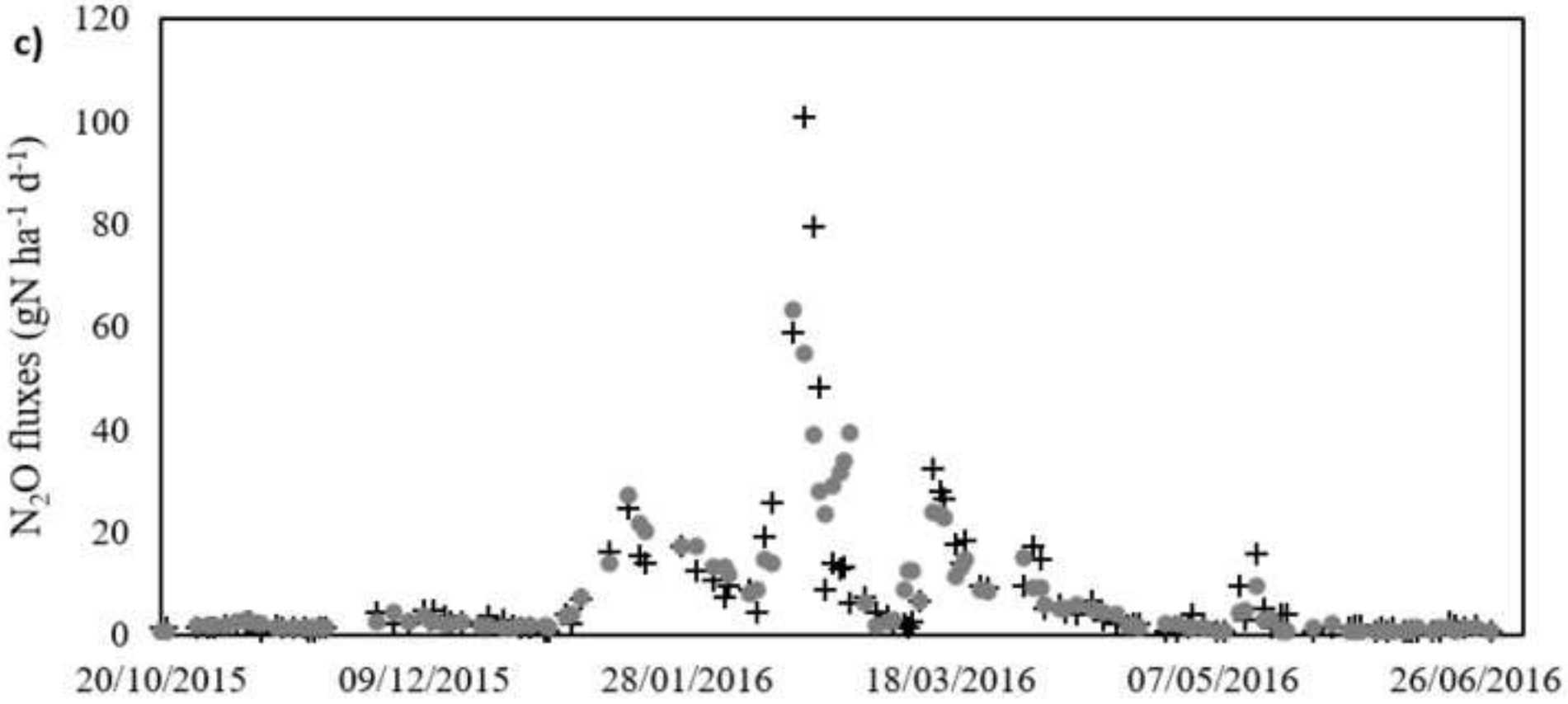
c)
120
100
80
60
40
20
0
N_2O fluxes (gN ha^{-1} d^{-1})
20/10/2015
09/12/2015
28/01/2016
18/03/2016
07/05/2016
26/06/2016

fig. 2.png

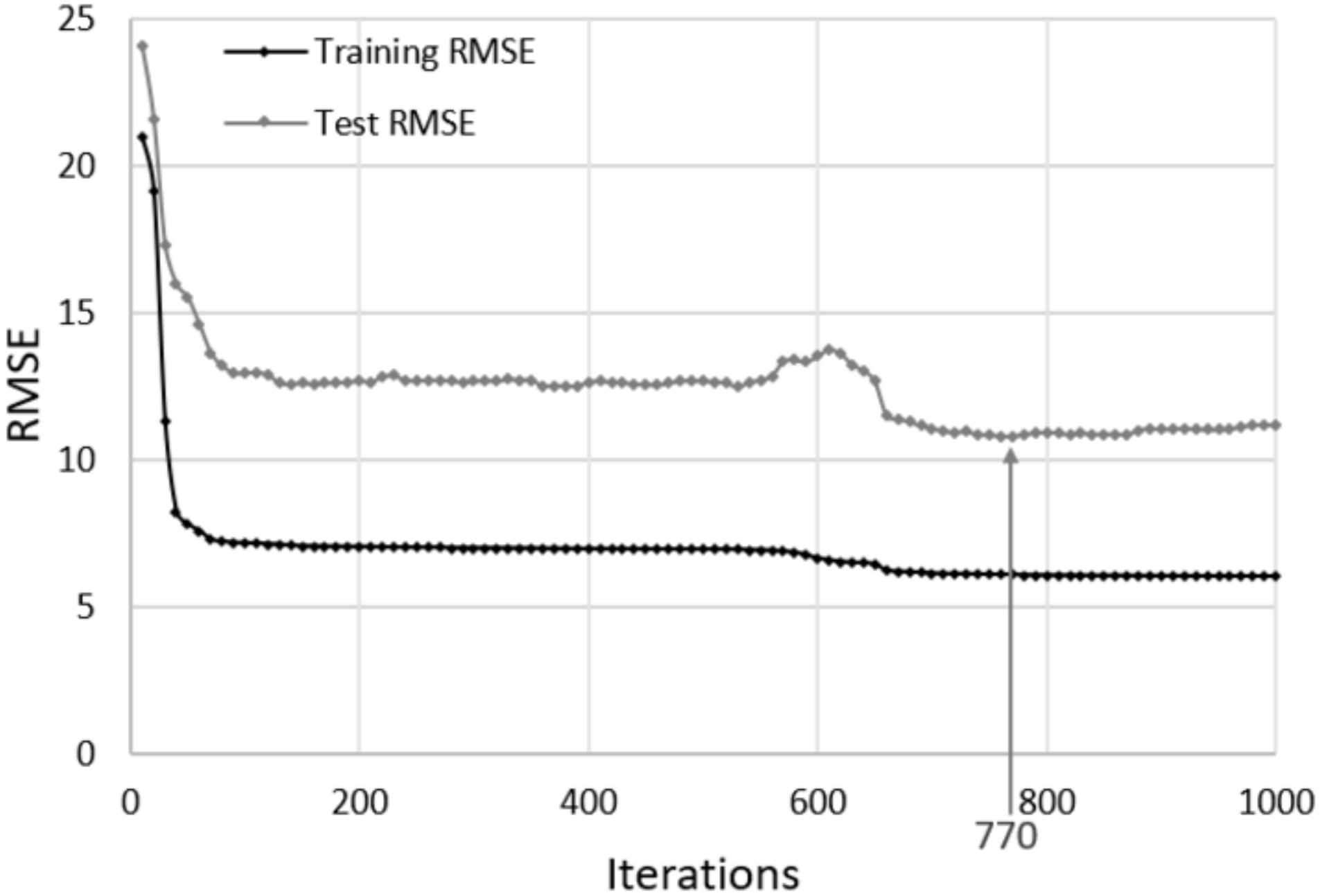
Training RMSE
Test RMSE
RMSE
25
20
15
10
5
0
0
200
400
600
800
1000
770
Iterations

fig. 3.png

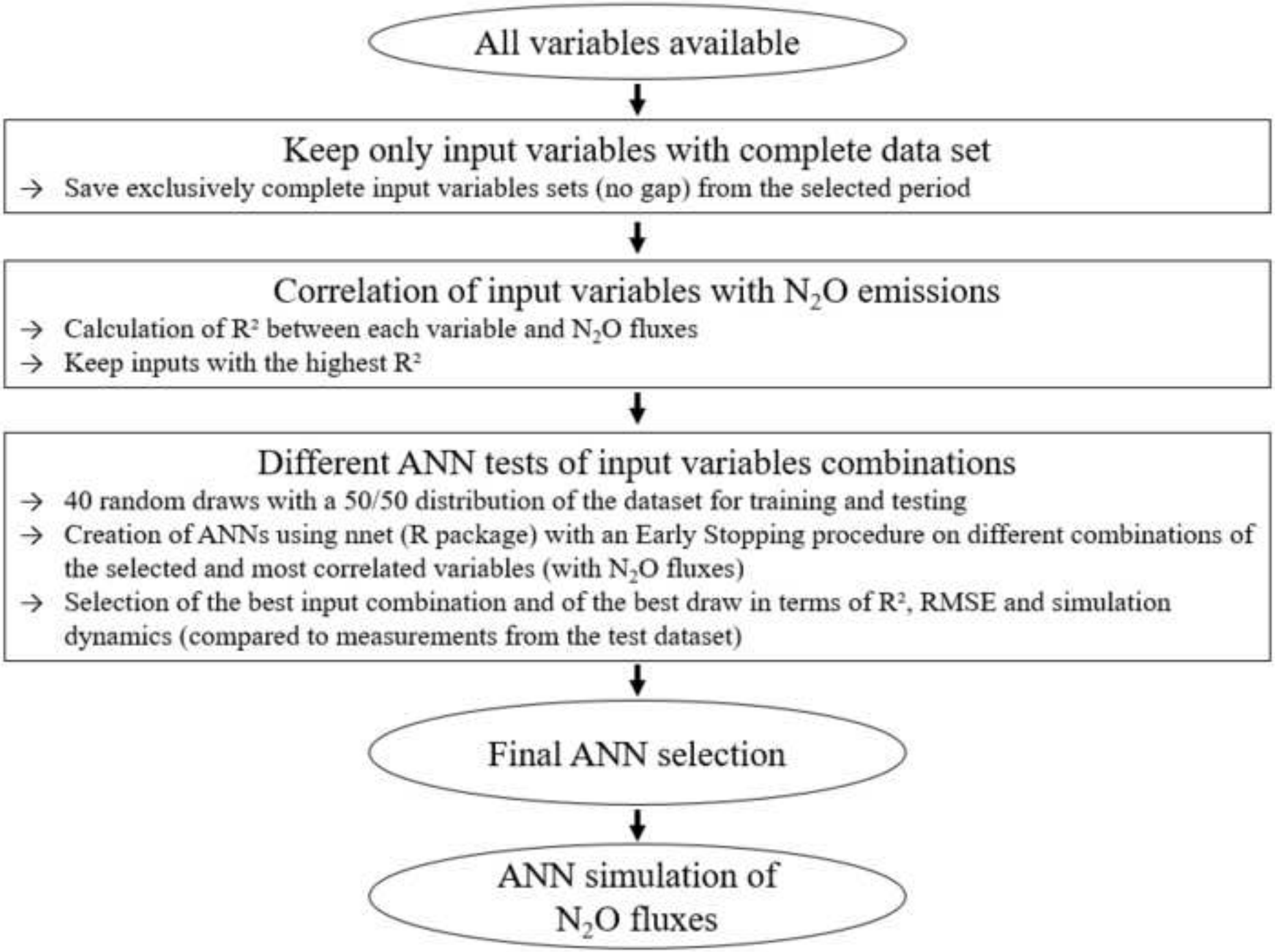
All variables available
Keep only input variables with complete data set
→ Save exclusively complete input variables sets (no gap) from the selected period
Correlation of input variables with N_2O emissions
→ Calculation of R^2 between each variable and N_2O fluxes
→ Keep inputs with the highest R^2
Different ANN tests of input variables combinations
→ 40 random draws with a 50/50 distribution of the dataset for training and testing
→ Creation of ANNs using nnet (R package) with an Early Stopping procedure on different combinations of the selected and most correlated variables (with N_2O fluxes)
→ Selection of the best input combination and of the best draw in terms of R^2, RMSE and simulation dynamics (compared to measurements from the test dataset)
Final ANN selection
ANN simulation of N_2O fluxes

fig. 4.png

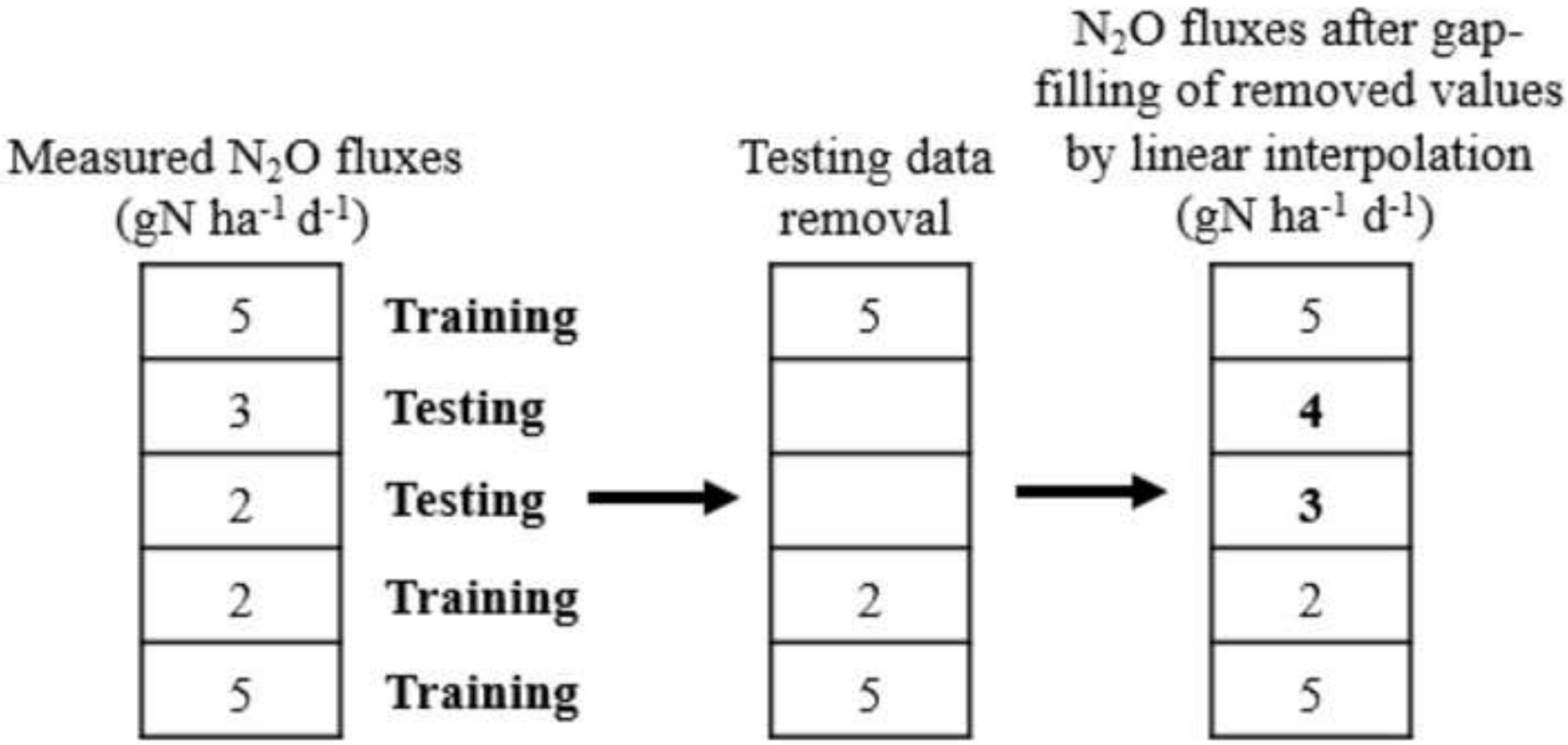
Measured N_2O fluxes (gN ha^{-1} d^{-1})
Testing data removal
N_2O fluxes after gap-filling of removed values by linear interpolation (gN ha^{-1} d^{-1})
5
Training
3
Testing
2
Testing
2
Training
5
Training
5
2
5
5
4
3
2
5

fig. 5.png

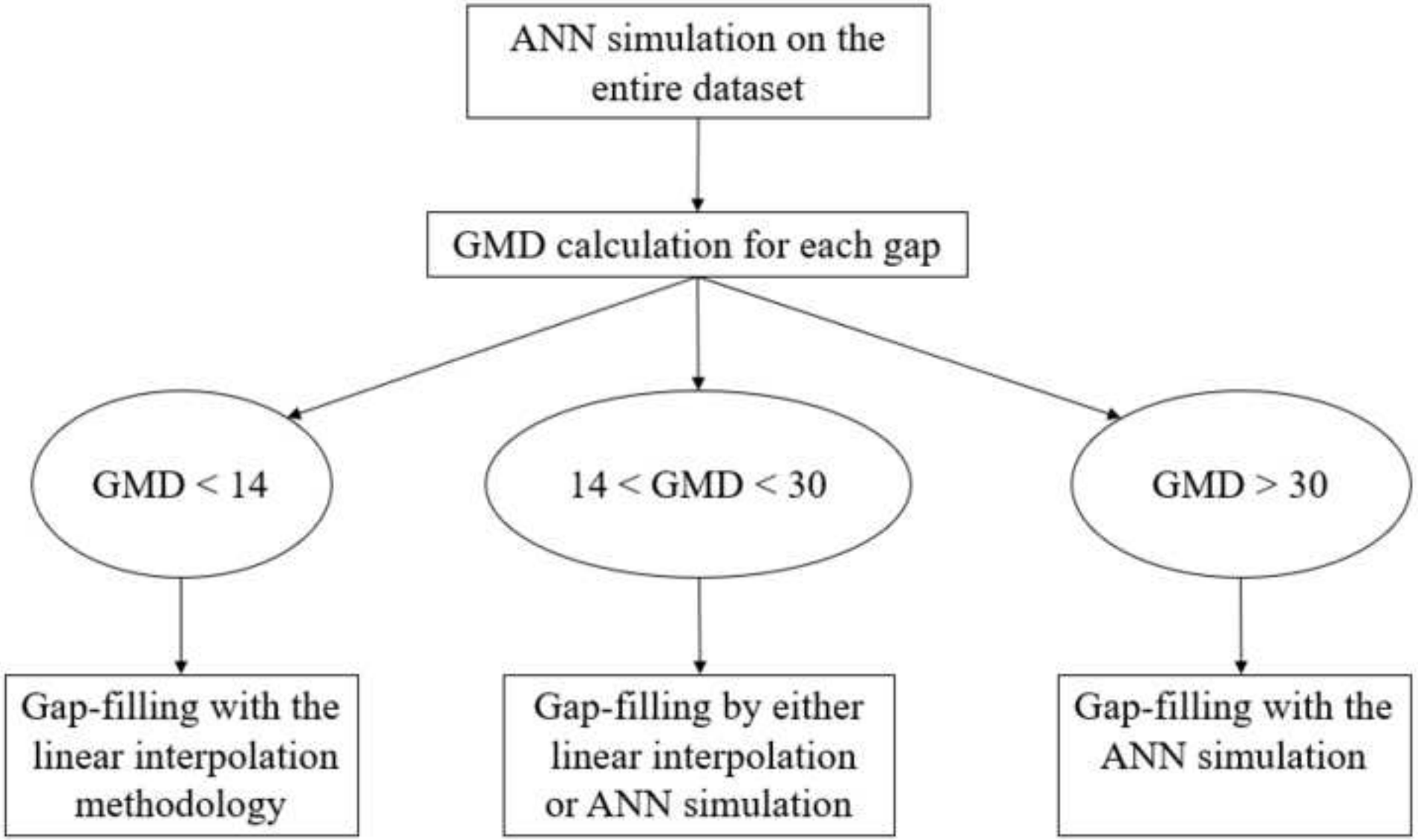
ANN simulation on the entire dataset
GMD calculation for each gap
GMD < 14
14 < GMD < 30
GMD > 30
Gap-filling with the linear interpolation methodology
Gap-filling by either linear interpolation or ANN simulation
Gap-filling with the ANN simulation

fig. 6.png

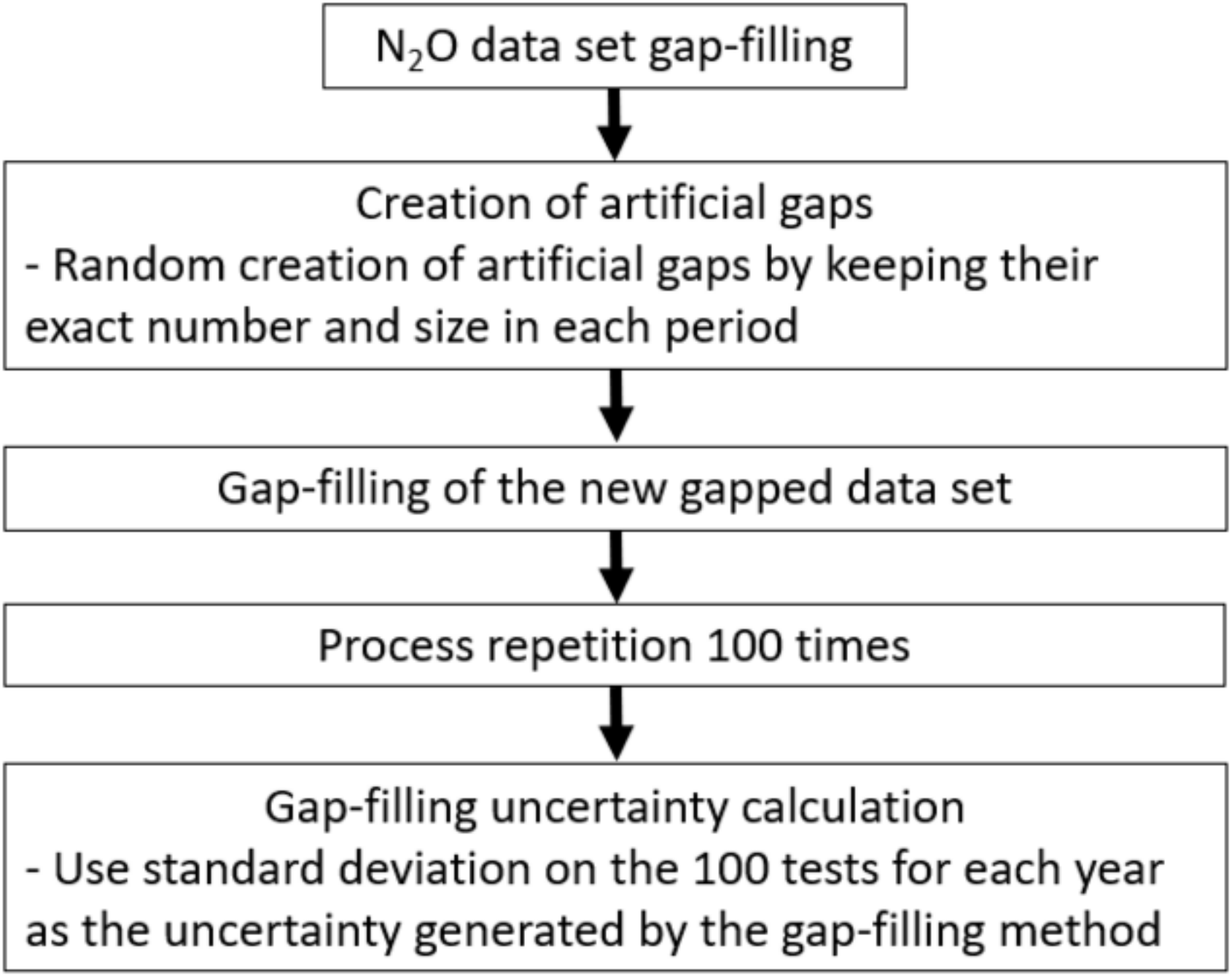
N_2O data set gap-filling
Creation of artificial gaps
- Random creation of artificial gaps by keeping their exact number and size in each period
Gap-filling of the new gapped data set
Process repetition 100 times
Gap-filling uncertainty calculation
- Use standard deviation on the 100 tests for each year as the uncertainty generated by the gap-filling method

fig. 7.png

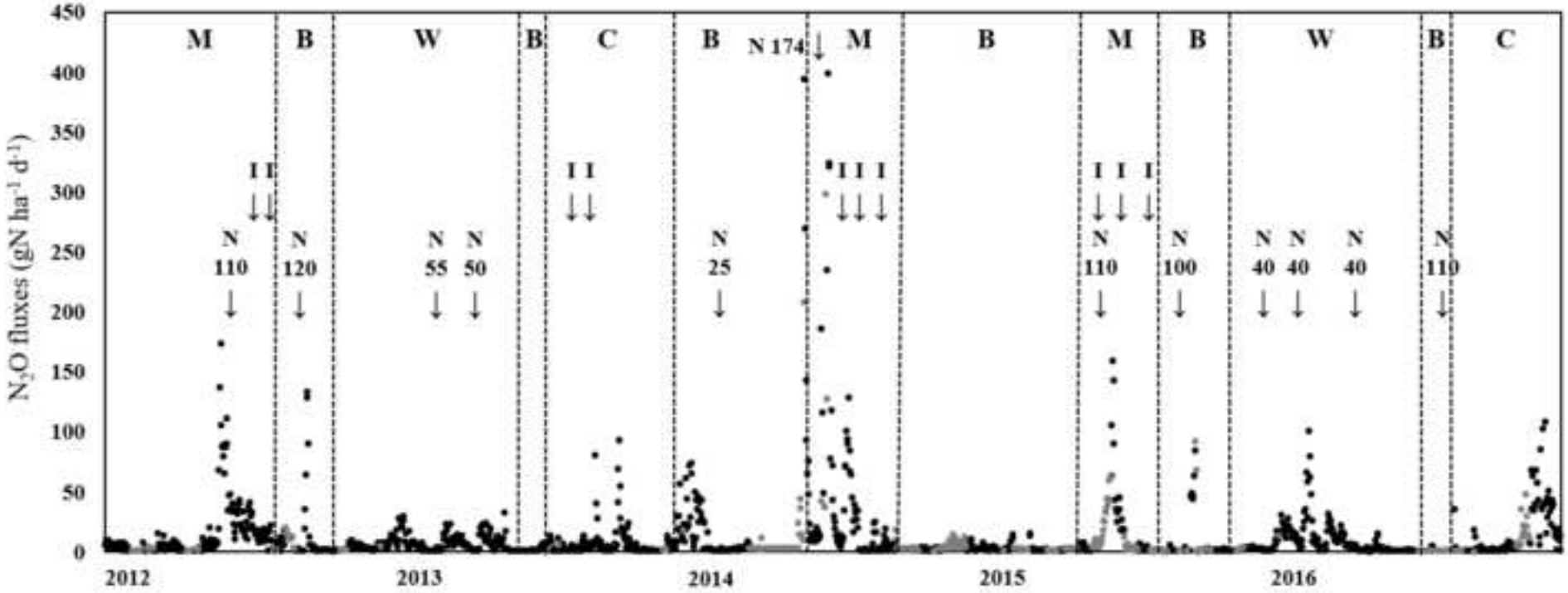
N2O fluxes (gN ha-1 d-1)
450
400
350
300
250
200
150
100
50
0
M
B
W
B
C
B
M
B
M
B
W
B
C
N 174
I I
I I I
I I I
I I
N 110
N 120
N 55
N 50
N 25
N 110
N 100
N 40
N 40
N 40
N 110
2012
2013
2014
2015
2016

fig. 8.png

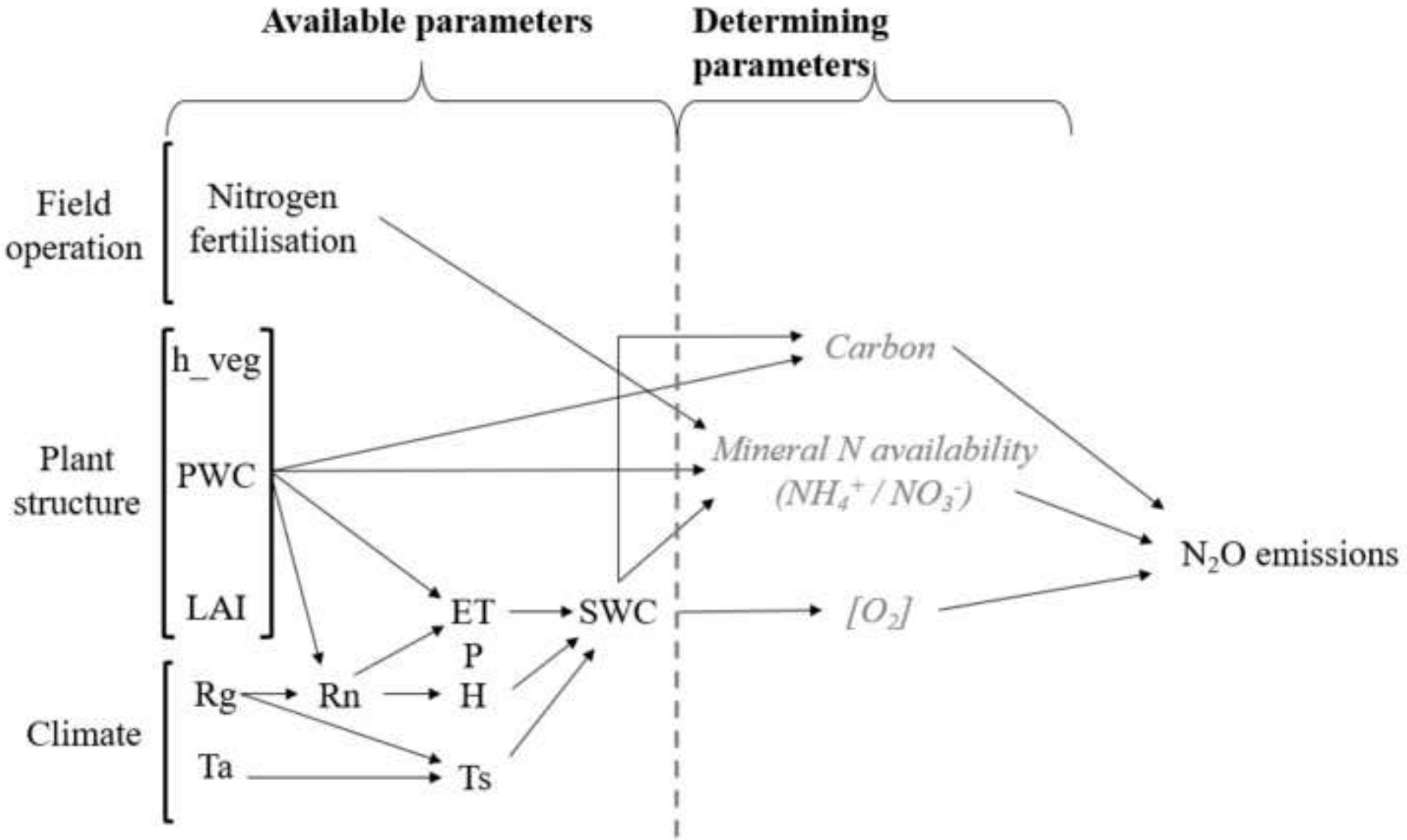
Available parameters
Determining parameters
Field operation
Nitrogen fertilisation
Plant structure
h_veg
PWC
LAI
Climate
Rg
Rn
Ta
ET
P
H
Ts
SWC
Carbon
Mineral N availability
(NH_4^+ / NO_3^-)
[O_2]
N_2O emissions

fig. 9.png

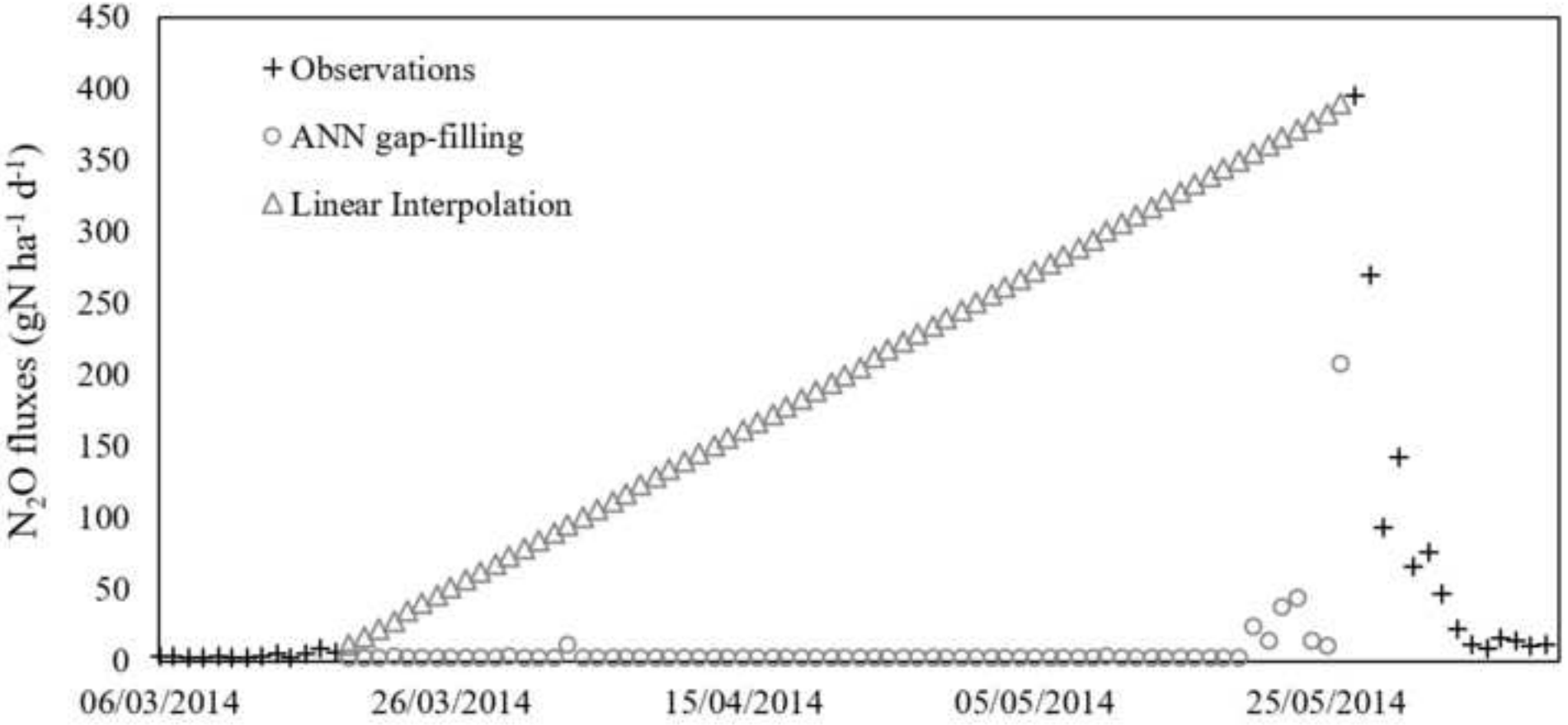
450
400
350
300
250
200
150
100
50
0
+ Observations
○ ANN gap-filling
△ Linear Interpolation
N_2O fluxes (gN ha^{-1} d^{-1})
06/03/2014
26/03/2014
15/04/2014
05/05/2014
25/05/2014